HHS Public Access

Author manuscript

Neurobiol Aging. Author manuscript; available in PMC 2021 September 01.

Published in final edited form as:

Neurobiol Aging. 2021 September ; 105: 99–114. doi:10.1016/j.neurobiolaging.2021.04.012.

Synaptic proteins associated with cognitive performance and neuropathology in older humans revealed by multiplexed fractionated proteomics

Becky C. Carlyle[a,b,*], **Savannah E. Kandigian**[a,b], **Johannes Kreuzer**[b,c], **Sudeshna Das**[a,b], **Bianca A. Trombetta**[a,b], **Yikai Kuo**[a,b,d], **David A. Bennett**[e], **Julie A. Schneider**[e], **Vladislav A. Petyuk**[f], **Robert R. Kitchen**[b,d], **Robert Morris**[b,c], **Angus C. Nairn**[g], **Bradley T. Hyman**[a,b], **Wilhelm Haas**[b,c], **Steven E. Arnold**[a,b]

[a]Massachusetts General Hospital Department of Neurology, Charlestown, MA, USA

[b]Harvard Medical School, Boston, MA, USA

[c]Massachusetts General Hospital Cancer Center, Charlestown, MA, USA

[d]Massachusetts General Hospital, Cardiology Division, Charlestown, MA, USA

[e]Rush Alzheimer's Disease Center, Chicago, IL, USA

[f]Pacific Northwest National Laboratory, Richland, WA, USA

[g]Yale Department of Psychiatry, New Haven, CT, USA

Abstract

Alzheimer's disease (AD) is defined by the presence of abundant amyloid-β (Aβ) and tau neuropathology. While this neuropathology is necessary for AD diagnosis, it is not sufficient for causing cognitive impairment. Up to one third of community dwelling older adults harbor intermediate to high levels of AD neuropathology at death yet demonstrate no significant cognitive impairment. Conversely, there are individuals who exhibit dementia with no gross explanatory neuropathology. In prior studies, synapse loss correlated with cognitive impairment. To understand how synaptic composition changes in relation to neuropathology and cognition, multiplexed liquid chromatography mass-spectrometry was used to quantify enriched synaptic proteins from the

[*]Corresponding author at: Massachusetts General Hospital Department of Neurology, 114 16th St, Charlestown, MA, 02129, USA. Phone: + 1 617 643 2640 bcarlyle@mgh.harvard.edu (B.C. Carlyle).

CRediT authorship contribution statement

Becky C. Carlyle: Conceptualization, Methodology, Formal analysis, Investigation, Data curation, Writing – original draft, Visualization. **Savannah E. Kandigian:** Investigation, Writing – review & editing. **Johannes Kreuzer:** Investigation. **Sudeshna Das:** Supervision. **Bianca A. Trombetta:** Validation, Writing – review & editing. **Yikai Kuo:** Formal analysis, Visualization, Data curation. **David A. Bennett:** Resources, Writing – review & editing, Conceptualization. **Julie A. Schneider:** Resources, Conceptualization. **Vladislav A. Petyuk:** Writing – review & editing, Supervision. **Robert R. Kitchen:** Formal analysis, Data curation, Supervision, Resources. **Robert Morris:** Data curation. **Angus C. Nairn:** Writing – review & editing, Supervision. **Bradley T. Hyman:** Writing – review & editing, Supervision, Resources. **Wilhelm Haas:** Resources, Data curation, Writing – review & editing, Funding acquisition. **Steven E. Arnold:** Conceptualization, Resources, Data curation, Writing – review & editing, Funding acquisition.

Disclosure statement

The authors declare no conflict of interest in relation to this publication.

Supplementary material

Supplementary material associated with this article can be found, in the online version, at doi: 10.1016/j.neurobiolaging.2021.04.012.

parietal association cortex of 100 subjects with contrasting levels of AD pathology and cognitive performance. 123 unique proteins were significantly associated with diagnostic category. Functional analysis showed enrichment of serotonin release and oxidative phosphorylation categories in normal (cognitively unimpaired, low neuropathology) and “resilient” (unimpaired despite AD pathology) individuals. In contrast, frail individuals, (low pathology, impaired cognition) showed a metabolic shift towards glycolysis and increased presence of proteasome subunits.

Keywords

Aging; Alzheimer’s disease; Angular gyrus; Cognition; Cognitive resilience; Neuroproteomics

1. Introduction

Alzheimer’s disease (AD) is the most common cause of dementia, affecting an estimated 35 million individuals worldwide (Alzheimers & Dementia, 2018). Although the presence of abundant amyloid-beta (Aβ) plaques and tau tangle neuropathology is required for the diagnosis of AD, studies of community-residing older adults have shown that up to one third of people with no measurable cognitive impairment at death harbor neuropathology that would be classified as intermediate to high likelihood of AD (D. A. Bennett et al., 2006; Schneider et al., 2007). AD pathology therefore may be necessary in the diagnostic definition of AD, but it is not sufficient for causing the cognitive and functional manifestations of AD. The maintenance of cognitive performance in the face of substantial AD pathology has been described as resilience or asymptomatic AD. The phenomenon is often attributed to cognitive or brain reserve and some presume it to be a preclinical stage of symptomatic AD dementia. It is poorly understood (Arnold et al., 2013; Au et al., 2012; D.A. Bennett et al., 2006; Gelber et al., 2012; Iacono et al., 2009; Johnson et al., 2020; O’Brien et al., 2009; Savva et al., 2009; Schneider et al., 2007). Conversely, some individuals show significant cognitive and functional impairments with aging despite absent or minimal AD pathology, cerebrovascular disease, or other neurodegenerative diseases in the brain. This cognitive frailty is even less well-studied.

Synapse loss has long been considered a strong correlate of cognitive impairment in AD (DeKosky and Scheff, 1990; Koffie et al., 2011; Terry et al., 1991). Clinicopathological studies of individuals enrolled in the Rush Religious Orders Study and Memory and Aging Project (ROSMAP) highlighted comparable pre-synaptic and post-synaptic staining levels in cognitively and pathologically normal individuals and resilient individuals (Bennett et al., 2018). Another study suggested resilient individuals have similar densities of thin and mushroom spines in the dorsolateral prefrontal cortex relative to controls (Boros et al., 2017). Proteomic studies of post-mortem cortical tissue from individuals with AD showed decreases in pre-synaptic SNAP25, Syntaxin 1A & B (STX1A & B), and synaptotagmin (SYT1), and the post-synaptic markers PSD95, disks large MAGUK scaffold protein 3 (DLG3), and Neuroligin 2 (NLGN2) (Johnson et al., 2020; Ping et al., 2018). Aged individuals with a worse cognitive trajectory have lower post-mortem levels of synaptic markers, including PSD95, SYT1, and STX1A (Wingo et al., 2019).

In a cytoarchitecturally complex tissue like the brain, interpreting sub-cellular- or organelle-specific protein composition or regulation from whole-tissue data may be confounded or obscured by global differences in sub-cellular compartment and organelle density or volume (Carlyle et al., 2017). In whole-tissue studies of AD, one of the strongest drivers of differential protein abundance is the general loss of neurons and synapses in AD cases compared to controls (Johnson et al., 2020, 2018; Ping et al., 2018; Wingo et al., 2019). Therefore, to better understand how protein composition within the synapse is affected in relation to AD pathology and cognition, we analyzed enriched synaptic fractions from brain tissue in ROSMAP samples by tandem mass tag labelled liquid chromatography mass-spectrometry (LC-MS3). Parietal association cortex (angular gyrus) tissue from 100 participants spanning four groups was analyzed: (1) cognitively unimpaired with low AD or other pathology (“Normal”), (2) dementia with high AD pathology (“Dementia-AD”), (3) “Resilient,” cognitively unimpaired despite high AD pathology, and (4) dementia without AD or any other attributable pathology “(Frail”). More than 100 proteins were significantly associated with diagnostic category, including important regulators of neurotransmitter release, metabolism, and protein degradation.

2. Materials and methods

2.1. Human brain tissue

Post-mortem tissue from the parietal association cortex (angular gyrus, Brodmann Area 39) was obtained from the Rush Alzheimer’s Disease Center. This region was chosen as an area of major interest in AD, lying at the heart of the temporoparietal association cortices showing hypometabolism in AD in decades of FDG-PET studies (Andriuta et al., 2016; Silverman et al., 2001), and dynamic ranges of Aβ and tau pathologies in the Braak staging spectrum for AD (Arnold et al., 1991; Braak and Braak, 1991). This avoids ceiling effects of entorhinal and hippocampal involvement and floor effects of primary sensory and motor cortices. Thus, it is ideal for defining low and high pathology groups. Tissue came from both the ROS and MAP projects (Bennett et al., 2018), similarly designed studies with longitudinal cohorts consisting of individuals who agreed to annual clinical evaluations and provided informed consent to donate their brains for research at the time of death. Annual evaluations included a medical history, neurological exam, and 21 cognitive tests assessing multiple cognitive domains that are commonly impaired in older individuals (Wilson et al., 2004, 2002). Cognitive scores were converted to Z-scores across the entire ROSMAP cohort and combined to generate a composite global cognition score. Brain autopsies were conducted with standardized protocols, including the preparation of diagnostic blocks for neuropathological classification according to NIA-Reagan, Braak, and CERAD staging. Case metadata is provided in Supplementary Table 1. Informed consent was obtained from all subjects, and tissue was obtained and analyzed under an Exempt Secondary Use protocol approved by the Massachusetts General Hospital Institutional Review Board (2016P001074).

2.2. Case selection and categorical grouping

In total, 100 cases that spanned the range of AD pathology and last valid global cognition scores in the ROSMAP cohorts were selected. These 100 cases were selected from 4

diagnostic bins stratified based on 2 variables. The first was the Braak Score, a 6-point scale that describes the brain-region specific pattern of AD pathology from early- to late-stage disease. Subjects were divided into low AD pathology (Braak Score of 4 or less) or high AD pathology (Braak Score of 5 or 6) on the basis of this variable. The second variable was a consensus clinical diagnosis from longitudinal cohort clinicians as to whether the subject was cognitively impaired at death. This decision was made using all available cognitive test data, with trajectory of global cognition score as the primary indicator. The global cognition score is a ROSMAP cohort-wide Z-score normalized summary value encompassing a battery of 21 different cognitive tests assessing 5 domains of cognition (episodic memory, semantic memory, working memory, perceptual orientation, and perceptual speed). Cases that showed incongruous findings in some cognitive domains were not included in the study. Samples were selected in quartets with the Frail sample (individuals with low AD pathology and cognitive impairment) as the reference case, given these were the least common diagnostic type in the cohort. This approach resulted in strong balancing for other key demographic variables including age, sex, education and post-mortem interval (Table 1) across four diagnostic groups of 25 subjects each.

2.3. Synaptic protein enrichment

Syn-PER Synaptic Protein Extraction Reagent (Thermo Fisher Scientific) was used to enrich for synaptic proteins from the frozen tissue samples. Complete Protease Inhibitor (EDTA Free, Roche) was added to the Syn-PER reagent (1 tablet per 50 ml). After removal of obvious white matter, approximately 100 mg of each frozen tissue piece was weighed, before adding 1 ml of Syn-PER per 100 mg of tissue and homogenization using 15 strokes of a Dounce homogenizer driven by a Scilogex OS-20S drive motor set at 500 rpm. Homogenates were centrifuged at 1,200 × g for 10 minutes at 4 °C. The supernatant (S1) was transferred to a new sample tube and centrifuged at 15,000 × g for 20 minutes at 4 °C. The supernatant (S2) was removed and discarded, and the resulting P2 pellet containing pre- and post-synaptic fractions and other membranous organelles was resuspended once in cold PBS to reduce contaminating proteins, before a second spin at 15,000 × g for 20 minutes at 4 °C. The washed P2 pellet was snap frozen and stored at −80 °C (see Fig. 2).

2.4. Multiplexed quantitative proteomics

P2 pellets were lysed by passing through a 21-gauge needle 20 times in 75 mM NaCl, 3% SDS, 1 mM NaF, 1 mM beta-glycerophosphate, 1 mM sodium orthovanadate, 10 mM sodium pyrophosphate, 1 mM PMSF and 1x Roche Complete Mini EDTA free protease inhibitors in 50 mM HEPES, pH 8.5. Lysates were then sonicated for 5 minutes in a sonicating water bath before cellular debris was pelleted by centrifugation at 14,000 rpm for 5 minutes. Proteins were reduced with dithiothreitol, alkylated with iodoacetamide (Edwards and Haas, 2016) and purified through methanolchloroform precipitation (Wessel and Flügge, 1984). Precipitated proteins were reconstituted in 1 M urea in 50 mM HEPES, pH 8.5, digested with 5 μg Lys-C and 5 μg trypsin, and desalted using C18 solid-phase extraction (SPE) (Sep-Pak, Waters). The concentration of the desalted peptide solutions was measured by BCA assay, and peptides were aliquoted into 50 μg portions. Peptide samples were allocated into 11 batches of 9 or 10 individual biological samples balanced by diagnostic condition, 1 or 2 pooled samples to be used to normalize for TMT labeling efficiency, plus

an 11th pooled bridge sample in each batch (Lapek et al., 2017).. Each batch was labeled with TMT11 as described previously (Edwards and Haas, 2016). Each of the pooled batches was desalted via C18 SPE and then fractionated into 12 fractions using Basic pH Reversed-Phase Liquid Chromatography (bRPLC), and individual fractions were analyzed by LC-MS3 (Edwards and Haas, 2016) (Fig. 1). TMT labels are isobaric in the first mass spectrometer (MS1), meaning the same peptide will coelute and be co-detected from all 11 samples. Upon fragmentation, the isobaric tags reveal different masses which are detected at MS2, enabling de-multiplexing of peptides from each sample contained in the pool and producing individual quantification data from each unique sample. Quantification after a further fragmentation (MS3 level) allows for quantification of each reporter ion alone, allowing for accurate and sensitive quantification (Ting et al., 2011a).

Twelve fractions from each TMT batch were analyzed by LC-MS2-MS3 on an Orbitrap Fusion mass spectrometer (Thermo Fisher Scientific) coupled to an Easy-nLC 1000 autosampler and HPLC system. Peptides were separated on an in-house pulled, in-house packed microcapillary column (inner diameter, 100 mm; outer diameter, 360 mm, 30 cm GP-C18, 1.8 mm, 120 Å, Sepax Technologies). Peptides were eluted with a linear gradient from 11 to 30% ACN in 0.125% formic acid over 165 minutes at a flow rate of 300 nL/min while the column was heated to 60 °C. Electrospray ionization was achieved by applying 1,500 V through a stainless-steel T-junction at the inlet of the microcapillary column.

The Orbitrap Fusion was operated in data-dependent mode using an LC-MS2/SPS-MS3 method. Full MS spectra were generated over an m/z range of 500–1,200 at a resolution of 6×10^4 with an Automatic Gain Control (AGC) setting of 5×10^5 and a maximum ion accumulation time of 100 msec. The most abundant ions detected in the survey scan were subjected to MS2 and MS3 experiments using the Top Speed setting that enables a maximum number of spectra to be acquired in a 5 sec experimental cycle before the next cycle is initiated with another survey full-MS scan. Ions for MS2 spectra were isolated in the quadrupole (0.5 m/z window), Collision Induced Dissociation (CID)-fragmented, and analyzed at rapid scan rate in the ion trap, where fragment ions were analyzed (AGC, 10×10^4; maximum ion accumulation time, 35 msec; normalized collision energy, 30%). MS3 analysis was performed using synchronous precursor selection (SPS-MS3) upon Higher Energy Collisional (HCD) fragmentation. Up to 10 MS2 precursors were simultaneously isolated and fragmented for MS3 analysis (isolation width, 2.5 m/z; AGC, 1×10^5; maximum ion accumulation time, 100 msec; normalized collision energy, 55%; resolution, 6×10^4). Fragment ions in the MS2 spectra with an m/z of 40 m/z below and 15 m/z above the precursor m/z were excluded from being selected for MS3 analysis.

2.5. Data processing

Data were processed using an in-house developed software suite (Huttlin et al., 2010). RAW files were converted into the mzXML format using a modified version of ReAdW.exe (http://www.ionsource.com/functional_reviews/readw/t2x_update_readw.htm). Spectral assignments of MS2 data were made using the Sequest algorithm (Eng et al., 1994) to search the Uniprot database (02/04/2014 release) of human protein sequences including known contaminants such as trypsin. The database included a decoy database consisting of all

protein sequences in reverse order (Elias and Gygi, 2007). Searches were performed with a 50 ppm precursor mass tolerance. Static modifications included 11-plex TMT tags on lysine residues and peptide N-termini (+229.162932 Da) and carbamidomethylation of cysteines (+57.02146 Da). Oxidation of methionine (+15.99492 Da) was included as a variable modification. Data were filtered to a peptide and protein false discovery rate of less than 1% using the targetdecoy search strategy (Elias and Gygi, 2007). This was achieved by first applying a linear discriminator analysis to filter peptide annotations using a combined score from the following peptide and spectral properties (Huttlin et al., 2010): XCorr, ΔCn, missed tryptic cleavages, peptide mass accuracy, and peptide length. The probability of a peptide-spectral match to be correct was calculated using a posterior error distribution and the probabilities of all peptides assigned to one specific protein were combined through multiplication. The dataset was re-filtered to a protein assignment FDR of less than 1% for the entire dataset of all proteins identified across all analyzed samples (Huttlin et al., 2010). Peptides that matched to more than one protein were assigned to that protein containing the largest number of matched redundant peptide sequences following the law of parsimony (Huttlin et al., 2010).

For quantitative analysis, TMT reporter ion intensities were extracted from the MS3 spectra by selecting the most intense ion within a 0.003 m/z window centered at the predicted m/z value for each reporter ion, and signal-to-noise (S/N) values were extracted from the RAW files. Spectra were used for quantification if the sum of the S/N values of all reporter ions was ≥ 440 and the isolation specificity for the precursor ion was ≥ 0.75. Protein intensities were calculated by summing the TMT reporter ions for all peptides assigned to a protein. Normalization of the quantitative data followed a multi-step process. Intensities were first normalized using the intensity measured for the bridge sample (Lapek et al., 2017). Taking account of slightly different protein amounts analyzed in each TMT channel, we then added an additional normalization step by normalizing the protein intensities measured for each sample by the global median of the per-sample median protein intensities (see Figure S3A, B).

2.6. Data analysis

Median-normalized protein quantifications were imported into R for all downstream analysis. All code used from this point forwards is provided in R project format, including.csv format supplementary tables. To resolve remaining variability (Figure S3A, B) in the median-normalized per-sample protein abundance distributions, we applied a full quantile normalization using the PreProcessCore R package. In building synaptic protein inclusion lists, protein ID conversion was performed using downloaded flat files from biomart (Smedley et al., 2015) (Mouse version: GRCm38.p6, Human version: GRCH38.p12) when necessary. The dataset was filtered twice; first to remove proteins with greater than 30% missing values, and second using an inclusion list of synaptic proteins. The inclusion list comprised 5667 proteins annotated as synaptic using the gene ontology (Ashburner et al., 2000), SynaptomeDB (Pirooznia et al., 2012), and Genes2Cognition databases, and proteins detected in the synaptic compartment in high quality proteomic studies (Bayés et al., 2014, 2011; Distler et al., 2014; Föcking et al., 2016; Li et al., 2017; Pandya et al., 2017) that employed a variety of purification techniques (density gradients,

immunoprecipitation of scaffolds, detergent extraction). For modeling, missing values (defined as NA in R) were replaced with the lowest detected value for that protein (Carlyle et al., 2017). Linear modelling, ANOVAs, Tukey HSD tests, and correction for multiple comparisons were performed using base R functions on log transformed data to satisfy assumptions of normality. The broom package was used to tidy modeling output. The ggsignif and scales packages were used in combination with ggplot for data plots. All boxplots are standard R ggplot format, with the median as the measure of center, box showing the interquartile range (IQR), and whiskers representing 1.5 times the IQR. All data points are shown on these plots. Files for input to GSEA (Subramanian et al., 2005) were prepared using a base R script. GSEA analyses were run using the java applet downloaded from http://software.broadinstitute.org/gsea/index.jsp, with downstream analysis and plotting performed in R. GSEA was performed using REACTOME version 7.2 ontology.

2.7. Data availability

Mass spectrometry RAW data are accessible through the MassIVE data repository (massive.ucsd.edu) under the accession number MSV000084959.

The code used to create all analyses, figures and supplementary tables for this manuscript can be found at: https://bitbucket.org/omicskitchen/tmtsynaptosomes.

Individual protein abundances across key variables can be explored at https://tmt-synaptosomes.omics.kitchen/.

3. Results and discussion

3.1. Sample demographics

Samples were classified into 4 diagnostic groups on the basis of 2 variables; the Braak score and clinical consensus of the presence of significant cognitive impairment at last study visit prior to death (Bennett et al., 2006) (Fig. 1 A). Twenty-five samples were allocated to each of the 4 groups; Normal (N) individuals with low AD pathology and no cognitive impairment, Dementia-AD (DEM_AD) individuals with high AD pathology and cognitive impairment, Resilient (RES) individuals with high AD pathology and no cognitive impairment, and Frail (FRL) individuals with low AD pathology and cognitive impairment. Key sample demographics were well matched across the 4 diagnostic categories including age at death, post-mortem interval (Fig. 1 B), sex, and education (Table 1).

One-way ANOVA with Tukey post-hoc testing showed that the global pathology score was significantly higher in the Dementia-AD and Resilient groups than the Normal and Frail groups (Fig. 1 B), and that the global cognition score at the last valid visit was significantly higher in the Normal and Resilient groups compared to the Frail and Dementia-AD groups (Fig. 1 B, Table S2). There was also a smaller significant difference in global cognition score between the Frail and Dementia-AD groups. The subjects were not selected for balanced ApoE status across groups, and thus this was not used as a variable in the downstream analysis. ApoE status distributed as expected across the groups (Figure S1). Although this variable was not included in the modeling, single protein data can be visualized relative to ApoE status at https://tmt-synaptosomes.omics.kitchen/. There were no consistent

enrichments for neuropathologies such as TDP-43, Lewy body and vascular pathologies in any group, including the Frail group (Figure S2).

3.2. Quantitative assessment of synaptic proteomes

Synaptic proteins were enriched from parietal association cortex using the Syn-PER Synaptic Protein Extraction Reagent (Fig. 1). Digested peptides were Tandem Mass Tag (TMT) labeled to be analyzed by LC-MS3. Prior to LC-MS3 analysis, each 11-plex was offline fractionated into 12 fractions by bRPLC to ensure deep coverage of the synaptic proteome, before analysis by SPS-MS3 (McAlister et al., 2014, 2012; Ting et al., 2011b) on an Orbitrap Fusion mass spectrometer (Fig. 2 A). Batch effects were mitigated by 2 step median scaling (Figure S3A,B). To resolve remaining variability in per-sample protein abundance distributions we applied a full quantile normalization and clustering showed no remaining batch effects (Figure S3C).

Across all individual samples, 9560 unique proteins were detected and quantified in at least one sample (Table S3). 6758 proteins remained after a filter was applied that removed proteins with over 30% missing values (Figure S4A), and 4952 proteins were detected in every sample. For modeling purposes, missing values were replaced with the lowest acquired value for that protein. Missing protein values were mostly related to batching structure and not diagnostic group (Figure S4A, B).

3.3. Enrichment and coverage of the synaptic proteome

General synapse loss has long been suggested as a strong predictor of cognitive decline in AD (DeKosky and Scheff, 1990; Koffie et al., 2011; Terry et al., 1991), as reflected in whole-tissue studies of AD (Johnson et al., 2020, 2018; Ping et al., 2018; Wingo et al., 2019). To avoid a volume effect-confound from synapse loss and to better enable identification of differential protein changes within synapses that were associated with cognitive performance, biochemically enriched synaptic fractions were analyzed. Biochemical enrichment also helps to reveal protein differences in synapses in two further ways. For some proteins, whole-tissue levels may mask a compartment-specific change; for example, we previously showed that synaptic enrichment was essential for detecting changes in PDE4A enzyme in the synapses from aged rodent cortex (Carlyle et al., 2014), with no change detectable at the whole-tissue level. Second, simplification of the protein mixture in the synaptic fraction allows greater sensitivity of the mass-spectrometer to lower abundance proteins.

Syn-PER enrichment was chosen as an enrichment method for two reasons: (1) once tissue is frozen without cryopreservation, membrane disruption prevents the preparation of pure organelle fractions (Dias et al., 2020); and (2) the protocol is simple and rapid compared to density gradient methods, reducing the potential introduction of variability in preparation methods in a large sample set. Cell fraction enrichment was assessed using human or mouse tissue proteomic studies (Bayés et al., 2014, 2011; Christoforou et al., 2016; Distler et al., 2014; Föcking et al., 2016; Foster et al., 2006; Itzhak et al., 2017; Li et al., 2017; Pirooznia et al., 2012; Thul et al., 2017) or Gene Ontology Cellular Compartment protein lists (Ashburner et al., 2000; The Gene Ontology Consortium, 2019). Proteins unique to any

fraction across these studies were used to assess enrichment or depletion by Bonferroni corrected Fisher tests. All fractions tested, except the nucleus (depleted, p.adj = $6.52e^{-14}$), were enriched (Figure S5), although cytoskeleton enrichment was not significant. The fractions with the strongest enrichment were post-synaptic (3.0-fold), and mitochondrial (2.3-fold, Table S4). There are far fewer proteomic studies of the pre-synapse than post-, and thus incomplete annotation of unique proteins may be part of the reason why this fraction appears less enriched here. All fractions found to be significantly enriched in this preparation have established presence in the pre- or post-synapse.

As the Syn-PER process is an enrichment and not a purification step, an important consideration for this technique, we applied a second bioinformatic filter to the proteins in the dataset using an inclusion list of 5667 synaptic proteins (see Methods). In total, we consistently detected 69% of the proteins from the inclusion list in this experiment. Moreover, we detected 532 proteins from the inclusion list that were not reported in a recent study of offline fractionated peptides from whole-tissue (Johnson et al., 2020). The inclusion list filter step resulted in a set of 3924 high-confidence synaptic proteins (Table S5) used for further modeling and analysis. Established general pre- and post-synaptic markers were plotted and assessed for protein abundance differences that may indicate gross synapse loss between groups. None of the established synaptic markers were significantly different between groups by one-way ANOVA (Fig. 2 B and C, Table S6), suggesting that the enrichment method used was successful in normalizing protein changes due to any bulk loss of synapses.

3.4. Analysis of diagnosis and synaptic protein abundance

Linear models were constructed with the 3924 proteins as outcome variables and diagnostic category, age, sex, education, and postmortem interval as explanatory variables. As expected, the majority of proteins that changed with post-mortem interval decreased as interval increased, likely a result of degraded peptides from protease activity. The small number of proteins that increased with interval may have lost a post-translational modification that made a peptide more detectable, or may have been more accessible to trypsin after protease activity in the tissue. A small number of proteins changed with age, including the neuropeptides SCG2 and VGF, and alpha-synuclein, which increased with age despite the fact that only 4 subjects in the study exhibited gross Lewy body pathology. Of the 34 proteins with sex differences, there were three members of the Annexin family, (IV, VI and VII) and two of the COPINE family (3 and 8), all of which were higher in females than males. These proteins are regulated by calcium levels, and in mice sex differences in calcium regulation and memory formation have been demonstrated related to oestrogen levels (Koss and Frick, 2017; Mizuno and Giese, 2010). It is of interest that these differences persist in human cortex long after these female subjects have passed menopause, as in unimpaired older adults, women tend to outperform men in episodic memory tasks (Ferreira et al., 2014; Herlitz et al., 1997). Only one protein, NRN1, was associated with both sex and diagnostic group, and was higher in males and lower in Dementia-AD compared to Normal.

A total of 123 unique proteins were significantly (FDR corrected $p < 0.05$) associated with diagnostic category. The group comparison with the largest number of significantly

associated proteins was the highest contrast diagnostic group comparison: Dementia-AD versus Normal, where 26 proteins were significantly increased in the Dementia-AD group versus Normal, while 71 were significantly decreased (summary Table 2, Table S7 for all protein data, Table S8 for significant only data across all model variables, including age, sex, and post-mortem interval, visualize individual proteins at https://tmt-synaptosomes.omics.kitchen/). Clustering Normal versus Dementia-AD samples on the basis of these proteins resulted in an extremely strong separation of the two groups (Fig. 3 A). The comparison between the Dementia-AD and Frail groups was also striking, with clustering on the basis of the 22 upregulated and 10 down-regulated proteins in the Frail group compared to Dementia-AD (Fig. 3 B), showing strong separation of the two groups. VGF, one of the most well replicated findings in proteomic studies of AD brain tissue and cerebrospinal fluid (Bai et al., 2020; Carlyle et al., 2018; Johnson et al., 2020), was strongly down-regulated in Dementia-AD compared to either of the Frail and Normal groups. For the remaining comparisons there were fewer significant proteins (Table 2), and the clustering was less consistent between the two groups (Fig. 3 C–F), suggesting that the presence of AD pathology in a sample drives a large proportion of the protein changes.

A sum of 17 proteins were significantly associated with more than one AD pathology contrast: AGAP2, AGRN, BAI2, CASKIN1, CEP170B, CPSF6, GK, GPR158, HSPB1, HTRA1, KCNAB1, KIAA1549, OLFM1, OLFM2, STK32C, VGF, and VPS39 (Fig. 3 G). Three were significant in three pathology contrasts (Fig. 4 A), with AGRN and CPSF6 being higher in subjects where AD pathology was high and STK32C being lower. Overall, there were fewer proteins associated with multiple cognitive status contrasts. Ten proteins were significantly associated with the Normal versus Frail comparison: ATP1B1, CCK, DGKG, HDGF, MTX2, NBAS, NOMO1, PDZRN3, PRMT8, TP53BP1 (Fig. 3 G, Fig. 4 B). ATP1B1 and NBAS were significantly higher in Normal subjects than both Dementia-AD and Frail subjects, while DGKG was lower in Normal subjects than both Dementia-AD and Frail subjects. HDGF was significantly higher in Frail subjects than Normal and Resilient subjects (Fig. 4 B). Only 3 proteins were significantly associated with the Resilient versus Dementia-AD subjects; LAP3, MACROD1, SEMA7A (Fig. 3 G, Fig. 4 C), with MACROD1 being lower in both Normal and Resilient subjects compared to those with Dementia-AD (Fig. 4 C).

Of the 123 proteins found to be significantly associated with diagnostic group, 53 of these proteins were previously identified in recent whole-tissue proteomic studies of the dorsolateral prefrontal cortex from Normal and AD brain samples (Bai et al., 2020; Johnson et al., 2020) (Table S8). These include the amyloid precursor protein APP, the now well established AD-associated proteins neurosecretory protein VGF (Beckmann et al., 2020) and complement 4B (Morgan, 2018), and NRN1 and HSPB1, which were identified in all three studies. AGAP2, identified by our study and the Johnson study, has been linked to AD by DNA methylation (Liu et al., 2019), and is a GTPase-activating protein with hundreds of network interactions in the post-synaptic compartment including scaffold proteins and protein kinases. These network interactions are enriched for proteins with known schizophrenia and autism spectrum disorder risk variants, both diseases having a cognitive component (Wilkinson et al., 2017). In contrast, PDE4A, a key cAMP regulating enzyme which we previously showed to be decreased at synapses in aging rhesus macaques (Carlyle

et al., 2014), was also revealed as lower in Dementia-AD subjects than Normal subjects in this study, but not in either of the other bulk tissues studies.

Of the proteins highlighted above which we believe may be novel human protein-level findings linked to AD, the AD pathology-related protein CPSF6 immunoprecipitates with a protein complex that regulates APP protein translation (Matthes et al., 2018), while HTRA1 is a serine protease that may be involved in APP processing (Grau et al., 2005). KCNAB1 mRNA changes have been shown to precede AD neuropathological changes in the dorsolateral prefrontal cortex (Bossers et al., 2010). Finally, the STK32C gene has DNA methylation changes that are associated with Braak staging (Gasparoni et al., 2018).

For proteins involved in cognitive contrasts, DGKG is a lipid kinase that interacts with multiple cellular signaling proteins to regulate the balance of diacylglycerol and phosphatidic acid (Shirai and Saito, 2014). HDGF has been identified at the transcriptional level as a possible protein interaction hub in AD (Hu et al., 2015), and mRNA abundance has been associated with expression of alternate tau splice variants (Chen et al., 2010). PRMT8 is an arginine methyltransferase that has been linked to stress tolerance in adult motor neurons (Simandi et al., 2018). Finally, SEMA7A is expressed in both neurons and oligodendrocytes, and is involved in signaling to oligodendrocyte precursors in the case of neuronal injury, and in signaling to T-cells and protection against reactive oxygen species (Quintremil et al., 2019). It is unclear why SEMA7A upregulation is seen in dementia-AD compared to resilient subjects, but it is striking that resilient subjects have the lowest SEMA7A levels of all four diagnostic groups (Fig. 4 C), suggesting a negative role in neurodegeneration for a protein that promotes axonal growth and branching during development (Pasterkamp and Giger, 2009).

The use of enrichment techniques in this study has therefore revealed a number of potential targets of interest for AD pathophysiology and non-AD related cognitive impairment that may have been obscured in whole-tissue studies. These novel findings may result from tissue fractionation revealing a subcellular compartment-specific change, from simplifying the mixture to allow identification of lower abundance proteins (Carlyle et al., 2018), or from a difference in cortical regions and disease stage analyzed. Compared to a previous whole tissue proteomic study of resilience versus dementia-AD (Johnson et al., 2020), we find fewer significant protein changes in this contrast in our study. This is partly due to a significant proportion of the proteins involved in this contrast in Johnson et al. 2020 arising from glial cells, particularly activated microglia. Johnson et al also saw a large depletion in general synaptic markers in dementia-AD, including DLG3, PSD95, SNAP25, SYN2, STX1A, and STX1B, suggesting the potential for a number of changes arising from bulk synaptic volume loss. Finally, our study was less well powered than the Johnson study, with an n of 25 per group compared to their 257 dementia-AD cases and 102 resilient cases. If we simulate an n = 50 study by doubling our sample set, significant findings in this contrast rise to 408 in the resilient versus dementia-AD contrast. While this is obviously an optimistic simulation, it clearly demonstrates that an increased sample size would likely increase the findings in this contrast. This is a clear limitation of the study and should be acknowledged for future projects such as this.

Gene set enrichment analysis; Dementia-AD versus Normal—To acknowledge the subtle biology and fully utilize proteins that may not have achieved strict significance following stringent FDR correction, we applied a non-parametric Gene Set Enrichment Analysis (GSEA) against the Reactome (v7.2) pathway database to examine functional differences between diagnostic groups. For the Dementia-AD versus Normal group, there were 190 significantly associated protein category terms (FDR q-value < 0.05, Table S9A). There was strong representation of proteasome subunit proteins in these terms, 44 of which were comprised of over 75% proteasome subunits (Table S9B). To reduce redundancy and aid interpretation we collapsed these into a single "Proteasome Enriched Terms" category. The enrichment of proteasome components in the synaptic enriched preparation is interesting, as studies of proteasome activity in brains from individuals with AD have generally shown decreased proteasome activity (Bonet-Costa et al., 2016). It is possible that proteasome components are upregulated in an attempt to regain proteostasis in the presence of misfolded oligomeric proteins that impair proteasome function (Thibaudeau et al., 2018). We also found that UCHL1, an immediate early gene and Ubiquitin C-terminal hydrolase enzyme necessary for synaptic plasticity, was significantly increased in Dementia-AD subjects versus Normal, in contrast to previous studies (Guglielmotto et al., 2017). It is therefore possible the timepoint of this study, during active disease, actually shows an initial localized upregulation of these proteins in an attempt to combat the insult of misfolded proteins and/or oxidative stress, or it may arise from a specific synaptic function, such as remodeling or elimination in response to signaling dysfunction, that is not identifiable in whole-tissue studies.

Clustering Dementia-AD and Normal samples on the basis of category Z-scores led to strong separation of samples by diagnostic category (Figure S6). Categories representing metabolism, particularly glycolysis and carbohydrate metabolism, were strongly enriched in Dementia-AD samples. Imaging studies using FDG-PET have suggested a shift in the bioenergetic profile of the brain during the onset of AD (Vlassenko and Raichle, 2015), with studies of non-neuronal primary cells from individuals with AD showing a shift towards energy production by glycolysis (Sonntag et al., 2017). We found TKT protein, which is essential for glycolysis, to be significantly upregulated in Dementia-AD versus Normal. Mitochondrial oxidative phosphorylation pathways were strongly enriched in the Normal subjects compared to Dementia-AD. Type II diabetes is one of the biggest comorbidities for dementia, and it is possible that insulin sensitivity may contribute to disruption in the balance of energy production pathways (Arnold et al., 2018), and that this metabolic dysregulation is a crucial facet of dementia pathophysiology.

3.5. Gene set enrichment analysis; Normal versus Frail

To identify categories related to cognitive impairment, GSEA was performed on the two diagnostic comparisons that were matched for AD pathology but divergent for cognitive performance. 81 categories were nominally significant (FDR q-value relaxed to < 0.1, Table S9C) in the Frail versus Normal comparison. Similar to above, 33 of these categories were comprised of over 75% proteasomal subunit proteins and these were again collapsed into one category, "Proteasome Enriched Terms." This category was enriched in Frail subjects, as were pathways related to glycolysis and carbohydrate metabolism (Fig. 5 A). In the absence

of any major molecular neuropathological lesions, the basis for proteasomal dysregulation, glycolysis and altered carbohydrate metabolism is interesting. We speculate that these individuals have a fundamental cellular-metabolic disease state distinct from (or prior to) the deposition of oligomeric or fibrillar proteins as disease-defining neuropathological features. There is substantial evidence in the literature that glucose utilization disturbances may precede the development of symptoms by up to a decade, which allows for a reasonable window for this to occur (reviewed Ryu et al., 2019), although in AD, such changes are typically detected after amyloid and tau.

Category terms related to protein translation machinery (with strong representation from ribosomal subunits themselves, Fig. 5 B, Table S9E) were unique to the Frail vs. Normal contrast. Previous reports have shown disturbances to ribosomal components in neurodegenerative diseases, overactive stress responses and defective regulatory responses (reviewed Delaidelli et al., 2019). The upregulation of ribosomal components in Frail subjects may therefore be an early step in protein translation dysfunction, or a compensatory response to oxidative stressors.

A further cluster containing the categories “SUMOylation”, “DNA Double Strand Break Repair”, and “MRNA Splicing” driven by the proteins DDX5, HNRNPC, HNRNPK, PARP1, and TP53BP1 was also unique to the Frail vs. Normal contrast. Individual proteins found to be differentially expressed are not well characterized, and only TP53BP1 is annotated in any of these categories, as described above (Fig. 5 B, Table S9D). Due to the usual nuclear localization of these proteins, we hypothesized these categories may reflect closer engagement and thus contamination from dividing cells such as microglia or astrocytes with the synaptic fraction in these subjects. However, there was no significant difference between diagnostic categories in the levels of astrocytic markers GFAP, ALDH1L1, and GLUL or the microglial marker CD11b (ITGAM) (Figure S7, Table S7).

Three clusters of categories were enriched in Normal subjects over Frail. First is a small cell adhesion cluster driven mostly by cadherin proteins, including cadherin2 (N-cadherin), which has been previously shown to be decreased in AD temporal cortex (Ando et al., 2011). Synaptic cell adhesion molecules are involved in establishing synapses, regulation of plasticity and synaptic remodeling (Leshchyns’Ka and Sytnyk, 2016), and loss of these molecules may be one of the precursors to synapse loss and cognitive dysfunction. A single “Respiratory Electron Transport” term was enriched in Normal individuals and shared with the Normal versus Dementia-AD contrast. The third cluster was unique to this contrast and contained the categories “Disassembly of Destruction Complex and Recruitment of AXIN to the Membrane” and “Signaling by WNT in Cancer,” and is driven by multiple Protein Phosphatase 2 subunits, GSK3β, and CTNNB1 (Fig. 5 A–C). Wnt signaling in the adult brain is involved in the clustering of scaffold proteins including PSD95, and spine morphogenesis. Multiple focused studies have found alterations in Wnt pathway components and downstream signaling pathways (Inestrosa and Varela-Nallar, 2014) in dementia.

3.6. Gene set enrichment analysis; Dementia vs. Resilient

The Dementia-AD versus Resilient comparison more closely reflected that of the Dementia-AD versus Normal (Fig. 6 A), indicating the high degree to which AD pathology is associated with synaptic composition. 111 protein categories were significant (FDR q-value < 0.05, Table S9E), with only 5 terms unique to this contrast (Fig. 5 C). Once again, we collapsed 19 pathways comprised of over 75% proteasome subunit proteins to one category. As seen with Normal subjects a smaller number of protein categories were enriched in unimpaired subjects. These included mitochondrial oxidative phosphorylation driven by NADH:Ubiquinone oxidoreductase proteins enriched in Resilience (Fig. 6 A cluster 10, 6B, Table S9F), suggesting a lack of the metabolic disturbances seen in the Dementia-AD and Frail subjects. “Serotonin Neurotransmitter Release Cycle” was also enriched in Resilient subjects. Given that depression is a risk factor and common feature of dementia, there has been interest in the serotonin system in the pathophysiology of dementia and in its treatment. A number of observational studies have suggested a beneficial effect of serotonin reuptake inhibitor use on cognitive decline (Mdawar et al., 2020), and a small imaging study showed lower levels of key serotonin transporters in MCI (Smith et al., 2017); proteins highlighted in this imaging study such as SERT were not detected in our study, and this would be an important topic for targeted follow up. In the opposite direction, metabolic processes such as carbohydrate metabolism and glycolysis were enriched in Dementia-AD compared to Resilient samples.

Two small immune clusters (Fig. 6 A, cluster 2 & 5) including generic categories such as adaptive and innate immunity were driven by protein phosphatase subunits, proteasomal subunits, CDC42, GRB2, MAPK1, and YES in Dementia-AD. The lack of specificity in these Reactome terms and the multi-functional nature of the proteins in neurons makes this finding difficult to contextualize in terms of the literature, although interest in neuroinflammation and neuron/glia interactions continues to grow (Heneka et al., 2015). Other immune categories (Fig. 6 A, grey font) enriched in Dementia-AD subjects were mostly driven by increased proteosomal subunits in the Dementia-AD subjects. This finding connects proteasomal upregulation to cognitive impairment and not the presence of AD pathology, given proteasomal subunits were upregulated in both Dementia-AD and Frail subjects, and depleted in Resilient subjects.

Finally, Dementia-AD subjects show an enrichment for a cluster of glutathione metabolic proteins (Fig. 6 A, cluster 9) compared to Resilient subjects. Glutathione levels have been of intermittent interest as AD biomarkers, with reports of depleted levels in AD brains and animal models of AD (Mandal et al., 2015; Saharan and Mandal, 2014). Glutathione is an antioxidant molecule, and the glutathione transferase proteins driving this category allow glutathione to conjugate to targets to detoxify and discharge them from the cell. Given the metabolic disturbances that are also enriched in the Dementia-AD subjects, it is unsurprising that a part of antioxidant system would also be dysregulated in neuronal sub-cellular compartments.

3.7. Study limitations

This work is a proteomic study of an enriched tissue fraction, and as such must be considered in the context of the strengths and weaknesses of this approach. Given the biochemical fractiona tion we used is an enrichment of synaptic proteins and not a purification, orthogonal validation of the synaptic relevance of these findings via immunohistochemistry would be of clear interest. This would be useful in the case of SEMA7A, for example, where it is possible that the increased signal from SEMA7A in dementia-AD compared to resilience may arise from contamination of the fraction with SEMA 7A expressing oligodendrocytes. This limitation could also be addressed using a synaptosomal or post-synaptic density preparation on a smaller number of samples, coupled with targeted LC-MS/MS or western blotting. To address this issue in our study, we used an inclusion list of proteins previously detected in the synaptic compartment using these more specific methods of biochemical fractionation. This list includes proteins with a synaptic and non-synaptic function, and is also not likely to be fully comprehensive, as it depends on the proteomic depth of the studies the lists are drawn from. For this reason, we have provided the option to explore all proteins on the companion website; https://tmt-synaptosomes.omics.kitchen/. A future goal for the field in general would be to unite such datasets and create a fully comprehensive synaptic proteome.

In this analysis we present a simple linear modelling approach which allows for accounting of other major demographic variables when assessing contrasts in diagnostic categories, with a relatively stringent adjusted p-value cut off for a proteomics study. The linear modeling is a reasonable choice for this study, with the majority of proteins meeting assumptions on the appropriate distribution of residuals. This modeling led to a small number of significant proteins in some diagnostic contrasts, such as resilient versus dementia-AD, likely as a result of experimental power discussed previously. In order to allow easy re-analysis of the data using other methods, or relaxation of adjusted p-values, we have provided all the required data in supplementary tables, including results from all proteins in the linear modeling (Table S7). For the ontology analysis, we chose GSEA as this method is based on protein ranking, and does not require a list of significant proteins. This approach is therefore better powered to compare these diagnostic groups, but may lead to a greater rate of false positive findings. Orthogonal follow up of key driver proteins, such as the SERT protein for serotonin signaling, would be an advisable next step for this work.

4. Conclusions

Using fractionated and TMT-labelled LS-MS3 proteomic analysis of biochemically and bioinformatically enriched synaptic proteins, we have highlighted proteins and pathways involved in cognitive resilience in the face of high levels of neuropathology, and cognitive frailty in individuals with minimal or no gross or microscopic neuropathology. Resilient subjects have low levels of LAP3, MACROD1, and SEMA7A proteins compared to Dementia-AD, an enrichment for “Serotonin Neurotransmitter Release Cycle,” metabolic categories enriched towards oxidative phosphorylation and depleted for glycolysis, and a depletion for proteasome enriched proteins and glutathione metabolic enzymes (see Fig. 7 for partial summary related to Frail vs. Resilient). For example, Frail individuals have

decreased ATP1B1, MTX2, NBAS, and PRMT8, and increased CCK, DGKG, HDGF, NOMO1, PDZRN3, and TP53BP1. They show metabolic shifts that are also observed in Dementia-AD, and accumulation of proteasome components, highlighting these shifts as critical for cognitive changes in dementia and not directly associated to AD pathology. Through this synapse-focused approach we have highlighted novel proteins that may be involved in the intersecting pathophysiologies that drive AD progression, and which may represent novel therapeutic targets or biomarkers of engagement for medications targeting inflammation, mitochondrial function, and synaptic modulation.

Supplementary Material

Refer to Web version on PubMed Central for supplementary material.

Acknowledgements

This work was supported by the Challenger Foundation / Minehan-Corrigan Family and by NIH R01 AG039478, R01 AG0 6230 6, P30 AG0 62421, R01 AG017917, P50 AG047270, P30 AG0 6 6508, R01 AG15819, P30 AG20262, R01 AG15819, R01 AG17917, and U01 AG61356. BCC is supported by the Bright Focus Foundation.

Abbreviations:

AD	Alzheimer's Disease
(Aβ)	amyloid-beta
LC-MS3	tandem mass tag labelled liquid chromatography mass-spectrometry with quantification at the MS3 level
TMT11	tandem mass tag labels, set of 11
bRPLC	Basic pH Reversed-Phase Liquid Chromatography
HPLC	high performance liquid chromatography
m/z	mass/charge
MMSE	Mini Mental State Examination
ROSMAP	Religious Orders Study & Memory and Aging Project
SPS-MS3	Synchronous Precursor Selection with MS3 scans
MS1, MS2, MS3	1st mass spectrometer, 2nd, 3rd
AGC	Automatic Gain Control
BA39	Brodmann Area 39
GSEA	Gene set enrichment analysis
FDG-PET	[^{18}F] fluorodeoxyglucose (FDG) positron emission tomography (PET)

SPE	Solid Phase Extraction

References

Alzheimers & Dementia, 2018. 2018 Alzheimer's disease facts and figures. Alzheimer's Dement 14, 367–429. doi: 10.1016/J.JALZ.2018.02.001.

Ando K, Uemura K, Kuzuya A, Maesako M, Asada-Utsugi M, Kubota M, Aoyagi N, Yoshioka K, Okawa K, Inoue H, Kawamata J, Shimohama S, Arai T, Takahashi R, Kinoshita A, 2011. N-cadherin regulates p38 MAPK signaling via association with JNK-associated leucine zipper protein: Implications for neurodegeneration in Alzheimer disease. J. Biol. Chem. doi: 10.1074/jbc.M110.158477.

Andriuta D, Moullart V, Schraen S, Devendeville A, Meyer ME, 2016. What are the most frequently impaired markers of neurodegeneration in ADNI subjects? J. Alzheimer's Dis. doi: 10.3233/JAD-150829.

Arnold SE, Arvanitakis Z, Macauley-Rambach SL, Koenig AM, Wang H-Y, Ahima RS, Craft S, Gandy S, Buettner C, Stoeckel LE, Holtzman DM, Nathan DM, 2018. Brain insulin resistance in type 2 diabetes and Alzheimer disease: concepts and conundrums. Nat. Rev. Neurol. 14, 168–181. doi: 10.1038/nrneurol.2017.185. [PubMed: 29377010]

Arnold SE, Hyman BT, Flory J, Damasio AR, Van Hoesen GW, 1991. The topographical and neuroanatomical distribution of neurofibrillary tangles and neuritic plaques in the cerebral cortex of patients with alzheimer's disease. Cereb. Cortex. doi: 10.1093/cercor/1.1.103.

Arnold SE, Louneva N, Cao K, Wang L-S, Han L-Y, Wolk DA, Negash S, Leurgans SE, Schneider JA, Buchman AS, Wilson RS, Bennett DA, 2013. Cellular, synaptic, and biochemical features of resilient cognition in Alzheimer's disease. Neurobiol. Aging 34, 157–168. doi: 10.1016/j.neurobiolaging.2012.03.004. [PubMed: 22554416]

Ashburner M, Ball CA, Blake JA, Botstein D, Butler H, Cherry JM, Davis AP, Dolinski K, Dwight SS, Eppig JT, Harris MA, Hill DP, Issel-Tarver L, Kasarskis A, Lewis S, Matese JC, Richardson JE, Ringwald M, Rubin GM, Sherlock G, 2000. Gene Ontology: tool for the unification of biology. Nat. Genet. 25, 25–29. doi: 10.1038/75556. [PubMed: 10802651]

Au R, Seshadri S, Knox K, Beiser A, Himali JJ, Cabral HJ, Auerbach S, Green RC, Wolf PA, McKee AC, 2012. The Framingham Brain Donation Program: neuropathology along the cognitive continuum. Curr. Alzheimer Res. 9, 673–686. [PubMed: 22471865]

Bai B, Wang X, Li Y, Chen PC, Yu K, Dey KK, Yarbro JM, Han X, Lutz BM, Rao S, Jiao Y, Sifford JM, Han J, Wang M, Tan H, Shaw TI, Cho JH, Zhou S, Wang H, Niu M, Mancieri A, Messler KA, Sun X, Wu Z, Pagala V, High AA, Bi W, Zhang H, Chi H, Haroutunian V, Zhang B, Beach TG, Yu G, Peng J, 2020. Deep Multilayer Brain Proteomics Identifies Molecular Networks in Alzheimer's Disease Progression. Neuron. 105, 975–991. doi: 10.1016/j.neuron.2019.12.015, e7. [PubMed: 31926610]

Bayés À, Collins MO, Galtrey CM, Simonnet C, Roy M, Croning MD, Gou G, van de Lagemaat LN, Milward D, Whittle IR, Smith C, Choudhary JS, Grant SG, 2014. Human post-mortem synapse proteome integrity screening for proteomic studies of postsynaptic complexes. Mol. Brain 88. doi: 10.1186/s13041-014-0088-4.

Bayés À, van de Lagemaat LN, Collins MO, Croning MDR, Whittle IR, Choudhary JS, Grant SGN, 2011. Characterization of the proteome, diseases and evolution of the human postsynaptic density. Nat. Neurosci. 14, 19–21. doi: 10.1038/nn.2719. [PubMed: 21170055]

Beckmann ND, Lin WJ, Wang M, Cohain AT, Charney AW, Wang P, Ma W, Wang YC, Jiang C, Audrain M, Comella PH, Fakira AK, Hariharan SP, Belbin GM, Girdhar K, Levey AI, Seyfried NT, Dammer EB, Duong D, Lah JJ, Haure-Mirande JV, Shackleton B, Fanutza T, Blitzer R, Kenny E, Zhu J, Haroutunian V, Katsel P, Gandy S, Tu Z, Ehrlich ME, Zhang B, Salton SR, Schadt EE, 2020. Multiscale causal networks identify VGF as a key regulator of Alzheimer's disease. Nat. Commun. doi: 10.1038/s41467-020-17405-z.

Bennett DA, Buchman AS, Boyle PA, Barnes LL, Wilson RS, Schneider JA, 2018. Religious orders study and rush memory and aging project. J. Alzheimers. Dis. 64, S161–S189. doi: 10.3233/JAD-179939. [PubMed: 29865057]

Bennett David A., Schneider JA, Aggarwal N, Arvanitakis Z, Shah RC, Kelly JF, Fox JH, Cochran EJ, Arends D, Treinkman AD, Wilson RS, 2006. Decision rules guiding the clinical diagnosis of Alzheimer's disease in two community-based cohort studies compared to standard practice in a clinic-based cohort study. Neuroepidemiology 27, 169–176. doi: 10.1159/000096129. [PubMed: 17035694]

Bennett DA, Schneider JA, Arvanitakis Z, Kelly JF, Aggarwal NT, Shah RC, Wilson RS, 2006. Neuropathology of older persons without cognitive impairment from two community-based studies. Neurology 66, 1837–1844. doi: 10.1212/01.wnl.0000219668.47116.e6. [PubMed: 16801647]

Bonet-Costa V, Pomatto LCD, Davies KJA, 2016. The proteasome and oxidative stress in Alzheimer's disease. Antioxid. Redox. Signal doi: 10.1089/ars.2016.6802.

Boros BD, Greathouse KM, Gentry EG, Curtis KA, Birchall EL, Gearing M, Herskowitz JH, 2017. Dendritic spines provide cognitive resilience against Alzheimer's disease. Ann. Neurol. 82, 602–614. doi: 10.1002/ana.25049. [PubMed: 28921611]

Bossers K, Wirz KTS, Meerhoff GF, Essing AHW, van Dongen JW, Houba P, Kruse CG, Verhaagen J, Swaab DF, 2010. Concerted changes in transcripts in the prefrontal cortex precede neuropathology in Alzheimer's disease. Brain. 133, 3699–3723. doi: 10.1093/brain/awq258. [PubMed: 20889584]

Braak H, Braak E, 1991. Neuropathological stageing of Alzheimer-related changes. Acta. Neuropathol 82, 239–259. [PubMed: 1759558]

Carlyle B, Trombetta B, Arnold S, 2018. Proteomic Approaches for the Discovery of Biofluid Biomarkers of Neurodegenerative Dementias. Proteomes. 6, 32. doi: 10.3390/proteomes6030032. [PubMed: 30200280]

Carlyle BC, Kitchen RR, Kanyo JE, Voss EZ, Pletikos M, Sousa AMM, Lam TT, Gerstein MB, Sestan N, Nairn AC, 2017. A multiregional proteomic survey of the postnatal human brain. Nat. Neurosci. 20, 1787–1795. doi: 10.1038/s41593-017-0011-2. [PubMed: 29184206]

Carlyle BC, Nairn AC, Wang M, Yang Y, Jin LE, Simen AA, Ramos BP, Bordner KA, Craft GE, Davies P, Pletikos M, Šestan N, Arnsten AFT, Paspalas CD, 2014. CAMP-PKA phosphorylation of tau confers risk for degeneration in aging association cortex. Proc. Natl. Acad. Sci. USA. 111. doi: 10.1073/pnas.1322360111.

Carlyle Becky C, Nairn AC, Wang M, Yang Y, Jin LE, Simen AA, Ramos BP, Bordner KA, Craft GE, Davies P, Pletikos M, Šestan N, Arnsten AFT, Paspalas CD., 2014. cAMP-PKA phosphorylation of tau confers risk for degeneration in aging association cortex. Proc. Natl. Acad. Sci. U. S. A. 111, 5036–5041. doi: 10.1073/pnas.1322360111. [PubMed: 24707050]

Chen S, Townsend K, Goldberg TE, Davies P, Conejero-Goldberg C, 2010. MAPT isoforms: Differential transcriptional profiles related to 3R and 4R splice variants. J. Alzheimer's Dis. doi: 10.3233/JAD-2010-101155.

Christoforou A, Mulvey CM, Breckels LM, Geladaki A, Hurrell T, Hayward PC, Naake T, Gatto L, Viner R, Arias AM, Lilley KS, 2016. A draft map of the mouse pluripotent stem cell spatial proteome. Nat. Commun. 7, 9992. doi: 10.1038/ncomms9992.

DeKosky ST, Scheff SW, 1990. Synapse loss in frontal cortex biopsies in Alzheimer's disease: Correlation with cognitive severity. Ann. Neurol. 27, 457–464. doi: 10.1002/ana.410270502. [PubMed: 2360787]

Delaidelli A, Jan A, Herms J, Sorensen PH, 2019. Translational control in brain pathologies: biological significance and therapeutic opportunities. Acta Neuropathol doi: 10.1007/s00401-019-01971-8.

Dias PRF, Gandra PG, Brenzikofer R, Macedo DV, 2020. Subcellular fractionation of frozen skeletal muscle samples. Biochem. Cell. Biol. 98, 293–298. doi: 10.1139/bcb-2019-0219. [PubMed: 31608669]

Distler U, Schmeisser MJ, Pelosi A, Reim D, Kuharev J, Weiczner R, Baumgart J, Boeckers TM, Nitsch R, Vogt J, Tenzer S, 2014. In-depth protein profiling of the postsynaptic density from mouse hippocampus using data-independent acquisition proteomics. Proteomics 14, 2607–2613. doi: 10.1002/pmic.201300520. [PubMed: 25211037]

Edwards A, Haas W, 2016. Multiplexed quantitative proteomics for high-throughput comprehensive proteome comparisons of human cell lines. Methods. Mol. Biol. 1394, 1–13. doi: 10.1007/978-1-4939-3341-9_1. [PubMed: 26700037]

Elias JE, Gygi SP, 2007. Target-decoy search strategy for increased confidence in large-scale protein identifications by mass spectrometry. Nat. Methods 4, 207–214. doi: 10.1038/nmeth1019. [PubMed: 17327847]

Eng JK, McCormack AL, Yates JR, 1994. An approach to correlate tandem mass spectral data of peptides with amino acid sequences in a protein database. J. Am. Soc. Mass Spectrom. 5, 976–989. doi: 10.1016/1044-0305(94)80016-2. [PubMed: 24226387]

Ferreira L, Ferreira Santos-Galduróz R, Ferri CP, Fernandes Galduróz JC, 2014. Rate of cognitive decline in relation to sex after 60 years-of-age: a systematic review. Geriatr. Gerontol. Int. 14, 23–31. doi: 10.1111/ggi.12093.

Föcking M, Dicker P, Lopez LM, Hryniewiecka M, Wynne K, English JA, Cagney G, Cotter DR, 2016. Proteomic analysis of the postsynaptic density implicates synaptic function and energy pathways in bipolar disorder. Transl. Psychiatry. 6, e959. doi: 10.1038/tp.2016.224. [PubMed: 27898073]

Foster LJ, de Hoog CL, Zhang Yanling, Zhang Yong, Xie X, Mootha VK, Mann M, 2006. A Mammalian Organelle Map by Protein Correlation Profiling. Cell. 125, 187–199. doi: 10.1016/j.cell.2006.03.022. [PubMed: 16615899]

Gasparoni G, Bultmann S, Lutsik P, Kraus TFJ, Sordon S, Vlcek J, Dietinger V, Steinmaurer M, Haider M, Mulholland CB, Arzberger T, Roeber S, Riemenschneider M, Kretzschmar HA, Giese A, Leonhardt H, Walter J, 2018. DNA methylation analysis on purified neurons and glia dissects age and Alzheimer's disease-specific changes in the human cortex. Epigenetics Chromatin doi: 10.1186/s13072-018-0211-3.

Gelber RP, Launer LJ, White LR, 2012. The Honolulu-Asia Aging Study: epidemiologic and neuropathologic research on cognitive impairment. Curr. Alzheimer Res. 9, 664–672. [PubMed: 22471866]

Grau S, Baldi A, Bussani R, Tian X, Stefanescu R, Przybylski M, Richards P, Jones SA, Shridhar V, Clausen T, Ehrmann M, 2005. Implications of the serine protease HtrA1 in amyloid precursor protein processing. Proc. Natl. Acad. Sci. U. S. A. doi: 10.1073/pnas.0501823102.

Guglielmotto M, Monteleone D, Vasciaveo V, Repetto IE, Manassero G, Tabaton M, Tamagno E, 2017. The decrease of Uch-L1 activity is a common mechanism responsible for A β 42 accumulation in Alzheimer's and vascular disease. Front. Aging. Neurosci. doi: 10.3389/fnagi.2017.00320.

Heneka MT, Carson MJ, Khoury J.El, Landreth GE, Brosseron F, Feinstein DL, Jacobs AH, Wyss-Coray T, Vitorica J, Ransohoff RM, Herrup K, Frautschy SA, Finsen B, Brown GC, Verkhratsky A, Yamanaka K, Koistinaho J, Latz E, Halle A, Petzold GC, Town T, Morgan D, Shinohara ML, Perry VH., Holmes C, Bazan NG, Brooks DJ, Hunot S, Joseph B, Deigendesch N, Garaschuk O, Boddeke E, Dinarello CA, Breitner JC, Cole GM, Golenbock DT, Kummer MP, 2015. Neuroinflammation in Alzheimer's disease. Lancet Neurol doi: 10.1016/S1474-4422(15)70016-5.

Herlitz A, Nilsson LG, Bäckman L, 1997. Gender differences in episodic memory. Mem. Cogn. 25, 801–811. doi: 10.3758/BF03211324.

Hu W, Lin X, Chen K, 2015. Integrated analysis of differential gene expression profiles in hippocampi to identify candidate genes involved in Alzheimer's disease. Mol. Med. Rep. doi: 10.3892/mmr.2015.4271.

Huttlin EL, Jedrychowski MP, Elias JE, Goswami T, Rad R, Beausoleil SA, Villén J, Haas W, Sowa ME, Gygi SP, 2010. A tissue-specific atlas of mouse protein phosphorylation and expression. Cell. 143, 1174–1189. doi: 10.1016/j.cell.2010.12.001. [PubMed: 21183079]

Iacono D, Markesbery WR, Gross M, Pletnikova O, Rudow G, Zandi P, Troncoso JC, 2009. The Nun study: clinically silent AD, neuronal hypertrophy, and linguistic skills in early life. Neurology. 73, 665–673. doi: 10.1212/WNL.0b013e3181b01077. [PubMed: 19587326]

Inestrosa NC, Varela-Nallar L, 2014. Wnt signaling in the nervous system and in Alzheimer's disease. J. Mol. Cell Biol. doi: 10.1093/jmcb/mjt051.

Itzhak DN, Davies C, Tyanova S, Mishra A, Williamson J, Antrobus R, Cox J, Weekes MP, Borner GHH, 2017. A mass spectrometry-based approach for mapping protein subcellular localization reveals the spatial proteome of mouse primary neurons. Cell. Rep 20, 2706–2718. doi: 10.1016/j.celrep.2017.08.063. [PubMed: 28903049]

Johnson ECB, Dammer EB, Duong DM, Ping L, Zhou M, Yin L, Higginbotham LA, Guajardo A, White B, Troncoso JC, Thambisetty M, Montine TJ, Lee EB, Trojanowski JQ, Beach TG, Reiman EM, Haroutunian V, Wang M, Schadt E, Zhang B, Dickson DW, Ertekin-Taner N, Golde TE, Petyuk VA, De Jager PL, Bennett DA, Wingo TS, Rangaraju S, Hajjar I, Shulman JM, Lah JJ, Levey AI, Seyfried NT, 2020. Large-scale proteomic analysis of Alzheimer's disease brain and cerebrospinal fluid reveals early changes in energy metabolism associated with microglia and astrocyte activation. Nat. Med. 26, 769–780. doi: 10.1038/s41591-020-0815-6. [PubMed: 32284590]

Johnson ECB, Dammer EB, Duong DM, Yin L, Thambisetty M, Troncoso JC, Lah JJ, Levey AI, Seyfried NT, 2018. Deep proteomic network analysis of Alzheimer's disease brain reveals alterations in RNA binding proteins and RNA splicing associated with disease. Mol. Neurodegener. 13, 52. doi: 10.1186/s13024-018-0282-4. [PubMed: 30286791]

Koffie RM, Hyman BT, Spires-Jones TL, 2011. Alzheimer's disease: synapses gone cold. Mol. Neurodegener. 6, 63. doi: 10.1186/1750-1326-6-63. [PubMed: 21871088]

Koss WA, Frick KM, 2017. Sex differences in hippocampal function. J. Neurosci. Res. 95, 539–562. doi: 10.1002/jnr.23864. [PubMed: 27870401]

Lapek JD, Greninger P, Morris R, Amzallag A, Pruteanu-Malinici I, Benes CH, Haas W, 2017. Detection of dysregulated protein-association networks by high-throughput proteomics predicts cancer vulnerabilities. Nat. Biotechnol. 35, 983–989. doi: 10.1038/nbt.3955. [PubMed: 28892078]

Leshchyns'Ka I, Sytnyk V, 2016. Synaptic cell adhesion molecules in Alzheimer's disease. Neural. Plast doi: 10.1155/2016/6427537.

Li J, Zhang W, Yang H, Howrigan DP, Wilkinson B, Souaiaia T, Evgrafov OV, Genovese G, Clementel VA, Tudor JC, Abel T, Knowles JA, Neale BM, Wang K, Sun F, Coba MP, 2017. Spatiotemporal profile of postsynaptic interactomes integrates components of complex brain disorders. Nat. Neurosci. 20, 1150–1161. doi: 10.1038/nn.4594. [PubMed: 28671696]

Liu Y, Wang M, Marcora EM, Zhang B, Goate AM, 2019. Promoter DNA hyper--methylation – Implications for Alzheimer's disease. Neurosci. Lett. doi: 10.1016/j.neulet.2019.134403.

Mandal PK, Saharan S, Tripathi M, Murari G, 2015. Brain Glutathione levels A novel biomarker for mild cognitive impairment and Alzheimer's disease. Biol. Psychiatry. doi: 10.1016/j.biopsych.2015.04.005.

Matthes F, Hettich MM, Schilling J, Flores-Dominguez D, Blank N, Wiglenda T, Buntru A, Wolf H, Weber S, Vorberg I, Dagane A, Dittmar G, Wanker E, Ehninger D, Krauss S, 2018. Inhibition of the MID1 protein complex: a novel approach targeting APP protein synthesis. Cell. Death. Discov doi: 10.1038/s41420-017-0003-8.

McAlister GC, Huttlin EL, Haas W, Ting L, Jedrychowski MP, Rogers JC, Kuhn K, Pike I, Grothe RA, Blethrow JD, Gygi SP, 2012. Increasing the multiplexing capacity of TMTs using reporter ion isotopologues with isobaric masses. Anal. Chem. 84, 7469–7478. doi: 10.1021/ac301572t. [PubMed: 22880955]

McAlister GC, Nusinow DP, Jedrychowski MP, Wühr M, Huttlin EL, Erickson BK, Rad R, Haas W, Gygi SP, 2014. MultiNotch MS3 enables accurate, sensitive, and multiplexed detection of differential expression across cancer cell line proteomes. Anal. Chem. 86, 7150–7158. doi: 10.1021/ac502040v. [PubMed: 24927332]

Mdawar B, Ghossoub E, Khoury R, 2020. Selective serotonin reuptake inhibitors and Alzheimer's disease. Neural. Regen. Res. doi: 10.4103/1673-5374.264445.

Mizuno K, Giese KP, 2010. Towards a molecular understanding of sex differences in memory formation. Trends. Neurosci doi: 10.1016/j.tins.2010.03.001.

Morgan BP, 2018. Complement in the pathogenesis of Alzheimer's disease. Semin. Immunopathol. doi: 10.1007/s00281-017-0662-9.

O'Brien RJ, Resnick SM, Zonderman AB, Ferrucci L, Crain BJ, Pletnikova O, Rudow G, Iacono D, Riudavets MA, Driscoll I, Price DL, Martin LJ, Troncoso JC, 2009. Neuropathologic studies of the Baltimore Longitudinal Study of Aging (BLSA). J. Alzheimers. Dis. 18, 665–675. doi: 10.3233/JAD-2009-1179. [PubMed: 19661626]

Pandya NJ, Koopmans F, Slotman JA, Paliukhovich I, Houtsmuller AB, Smit AB, Li KW, 2017. Correlation profiling of brain sub-cellular proteomes reveals co-assembly of synaptic proteins and

subcellular distribution. Sci. Rep. 7, 12107. doi: 10.1038/s41598-017-11690-3. [PubMed: 28935861]

Pasterkamp RJ, Giger RJ, 2009. Semaphorin function in neural plasticity and disease. Curr. Opin. Neurobiol. doi: 10.1016/j.conb.2009.06.001.

Ping L, Duong DM, Yin L, Gearing M, Lah JJ, Levey AI, Seyfried NT, 2018. Global quantitative analysis of the human brain proteome in Alzheimer's and Parkinson's. Disease. Sci. Data 5, 180036. doi: 10.1038/sdata.2018.36.

Pirooznia M, Wang T, Avramopoulos D, Valle D, Thomas G, Huganir RL, Goes FS, Potash JB, Zandi PP, 2012. SynaptomeDB: an ontology-based knowledgebase for synaptic genes. Bioinformatics. 28, 897–899. doi: 10.1093/bioinformatics/bts040. [PubMed: 22285564]

Quintremil S, Ferrer Medina, F., Puente J, Elsa Pando M, Antonieta Valenzuela, 2019. Roles of semaphorins in neurodegenerative diseases. Neurons - Dendrites and Axons doi: 10.5772/intechopen.82046.

Ryu JC, Zimmer ER, Rosa-Neto P, Yoon SO, 2019. Consequences of metabolic disruption in Alzheimer's disease pathology. Neurotherapeutics doi: 10.1007/s13311-019-00755-y.

Saharan S, Mandal PK, 2014. The emerging role of glutathione in alzheimer's disease. J. Alzheimer's Dis. doi: 10.3233/JAD-132483.

Savva GM, Wharton SB, Ince PG, Forster G, Matthews FE, Brayne C, 2009. Age, Neuropathology, and Dementia. N. Engl. J. Med. 360, 2302–2309. doi: 10.1056/NEJMoa0806142. [PubMed: 19474427]

Schneider JA, Arvanitakis Z, Bang W, Bennett DA, 2007. Mixed brain pathologies account for most dementia cases in community-dwelling older persons. Neurology. 69, 2197–2204. doi: 10.1212/01.wnl.0000271090.28148.24. [PubMed: 17568013]

Shirai Y, Saito N, 2014. Diacylglycerol kinase as a possible therapeutic target for neuronal diseases. J. Biomed. Sci. doi: 10.1186/1423-0127-21-28.

Silverman DHS, Chen W, Czernin J, Kowell AP, Gambhir SS, Phelps ME, Lu CS, Aburto, Kung de MAK, Chang CY, Small GW, Cummings JL, Chen W, Rapoport SI, Pietrini P, Alexander GE, Schapiro MB, Pietrini P, Jagust WJ, Hoffman JM, Welsh-Bohmer KA, Alavi A, Clark CM, Salmon E, De Leon MJ, Mielke R, Hoh CK, 2001. Positron emission tomography in evaluation of dementia: Regional brain metabolism and long-term outcome. J. Am. Med. Assoc. doi: 10.1001/jama.286.17.2120.

Simandi Z, Pajer K, Karolyi K, Sieler T, Jiang LL, Kolostyak Z, Sari Z, Fekecs Z, Pap A, Patsalos A, Contreras GA, Reho B, Papp Z, Guo X, Horvath A, Kiss G, Keresztessy Z, Vámosi G, Hickman J, Xu H, Dormann D, Hortobagyi T, Antal M, Nógrádi A, Nagy L, 2018. Arginine methyltransferase PRMT8 provides cellular stress tolerance in aging motoneurons. J. Neurosci. doi: 10.1523/JNEUROSCI.3389-17.2018.

Smedley D, Haider S, Durinck S, Pandini L, Provero P, Allen J, Arnaiz O, Awedh MH, Baldock R, Barbiera G, Bardou P, Beck T, Blake A, Bonierbale M, Brookes AJ, Bucci G, Buetti I, Burge S, Cabau C, Carlson JW, Chelala C, Chrysostomou C, Cittaro D, Collin O, Cordova R, Cutts RJ, Dassi E, Genova ADi, Djari A, Esposito A, Estrella H, Eyras E FernandezBanet J, Forbes S, Free RC, Fujisawa T, Gadaleta E, Garcia-Manteiga JM, Goodstein D, Gray K, Guerra-Assunção JA, Haggarty B, Han D-J, Han BW, Harris T, Harshbarger J, Hastings RK, Hayes RD, Hoede C, Hu S, Hu ZL, Hutchins L, Kan Z, Kawaji H, Keliet A, Kerhornou A, Kim S, Kinsella R, Klopp C, Kong L, Lawson D, Lazarevic D, Lee J-H, Letellier T, Li C-Y, Lio P, Liu C-J, Luo J, Maass A, Mariette J, Maurel T, Merella S, Mohamed AM, Moreews F, Nabihoudine I, Ndegwa N, Noirot C, Perez-Llamas C, Primig M, Quattrone A, Quesneville H, Rambaldi D, Reecy J, Riba M, Rosanoff S, Saddiq AA, Salas E, Sallou O, Shepherd R, Simon R, Sperling L, Spooner W, Staines DM, Steinbach D, Stone K, Stupka E, Teague JW, Ullah, Dayem AZ, Wang J, Ware D, Wong-Erasmus M, Youens-Clark K, Zadissa A, Zhang S-J, Kasprzyk A, 2015. The BioMart community portal: an innovative alternative to large, centralized data repositories. Nucleic Acids Res 43, W589–W598. doi: 10.1093/nar/gkv350. [PubMed: 25897122]

Smith GS, Barrett FS, Joo JH, Nassery N, Savonenko A, Sodums DJ, Marano CM, Munro CA, Brandt J, Kraut MA, Zhou Y, Wong DF, Workman CI, 2017. Molecular imaging of serotonin degeneration in mild cognitive impairment. Neurobiol. Dis. doi: 10.1016/j.nbd.2017.05.007.

Sonntag KC, Ryu WI, Amirault KM, Healy RA, Siegel AJ, McPhie DL, Forester B, Cohen BM, 2017. Late-onset Alzheimer's disease is associated with inherent changes in bioenergetics profiles. Sci. Rep. doi: 10.1038/s41598-017-14420-x.

Subramanian A, Tamayo P, Mootha VK, Mukherjee S, Ebert BL, Gillette MA, Paulovich A, Pomeroy SL, Golub TR, Lander ES, Mesirov JP, 2005. Gene set enrichment analysis: a knowledge-based approach for interpreting genome-wide expression profiles. Proc. Natl. Acad. Sci. U. S. A. 102, 15545–15550. doi: 10.1073/pnas.0506580102. [PubMed: 16199517]

Terry RD, Masliah E, Salmon DP, Butters N, DeTeresa R, Hill R, Hansen LA, Katzman R, 1991. Physical basis of cognitive alterations in alzheimer's disease: Synapse loss is the major correlate of cognitive impairment. Ann. Neurol. 30, 572–580. doi: 10.1002/ana.410300410. [PubMed: 1789684]

The Gene Ontology Consortium, 2019. The Gene Ontology Resource: 20 years and still GOing strong. Nucleic. Acids. Res 47, D330–D338. doi: 10.1093/nar/gky1055. [PubMed: 30395331]

Thibaudeau TA, Anderson RT, Smith DM, 2018. A common mechanism of proteasome impairment by neurodegenerative disease-associated oligomers. Nat. Commun. doi: 10.1038/s41467-018-03509-0.

Thul PJ, Akesson L, Wiking M, Mahdessian D, Geladaki A, Ait Blal H, Alm T, Asplund A, Björk L, Breckels LM, Bäckström A, Danielsson F, Fagerberg L, Fall J, Gatto L, Gnann C, Hober S, Hjelmare M, Johansson F, Lee S, Lindskog C, Mulder J, Mulvey CM, Nilsson P, Oksvold P, Rockberg J, Schutten R, Schwenk JM, Sivertsson A, Sjöstedt E, Skogs M, Stadler C, Sullivan DP, Tegel H, Winsnes C, Zhang C, Zwahlen M, Mardinoglu A, Pontén F, von Feilitzen K, Lilley KS, Uhlén M, Lundberg E, 2017. A subcellular map of the human proteome. Science. 356 (80-.), eaal3321. doi: 10.1126/science.aal3321.

Ting L, Rad R, Gygi SP, Haas W, 2011a. MS3 eliminates ratio distortion in isobaric multiplexed quantitative proteomics. Nat. Methods 8, 937–940. doi: 10.1038/nmeth.1714. [PubMed: 21963607]

Ting L, Rad R, Gygi SP, Haas W, 2011b. MS3 eliminates ratio distortion in isobaric multiplexed quantitative proteomics. Nat. Methods 8, 937–940. doi: 10.1038/nmeth.1714. [PubMed: 21963607]

Vlassenko AG, Raichle ME, 2015. Brain aerobic glycolysis functions and Alzheimer's disease. Clin. Transl. imaging 3, 27. doi: 10.1007/S40336-014-0094-7. [PubMed: 26855936]

Wessel D, Flügge UI, 1984. A method for the quantitative recovery of protein in dilute solution in the presence of detergents and lipids. Anal. Biochem. 138, 141–143. doi: 10.1016/0003-2697(84)90782-6. [PubMed: 6731838]

Wilkinson B, Li J, Coba MP, 2017. Synaptic GAP and GEF complexes cluster proteins essential for GTP signaling. Sci. Rep. doi: 10.1038/s41598-017-05588-3.

Wilson RS, Bienias JL, Evans DA, Bennett DA, 2004. Religious orders study: Overview and change in cognitive and motor speed. Aging. Neuropsychol. Cogn. 11, 280–303. doi: 10.1080/13825580490511125.

Wilson RS, Mendes De Leon CF, Barnes LL, Schneider JA, Bienias JL, Evans DA, Bennett DA, 2002. Participation in cognitively stimulating activities and risk of incident Alzheimer disease. JAMA. 287, 742–748. [PubMed: 11851541]

Wingo AP, Dammer EB, Breen MS, Logsdon BA, Duong DM, Troncosco JC, Thambisetty M, Beach TG, Serrano GE, Reiman EM, Caselli RJ, Lah JJ, Seyfried NT, Levey AI, Wingo TS, 2019. Large-scale proteomic analysis of human brain identifies proteins associated with cognitive trajectory in advanced age. Nat. Commun. 10, 1619. doi: 10.1038/s41467-019-09613-z. [PubMed: 30962425]

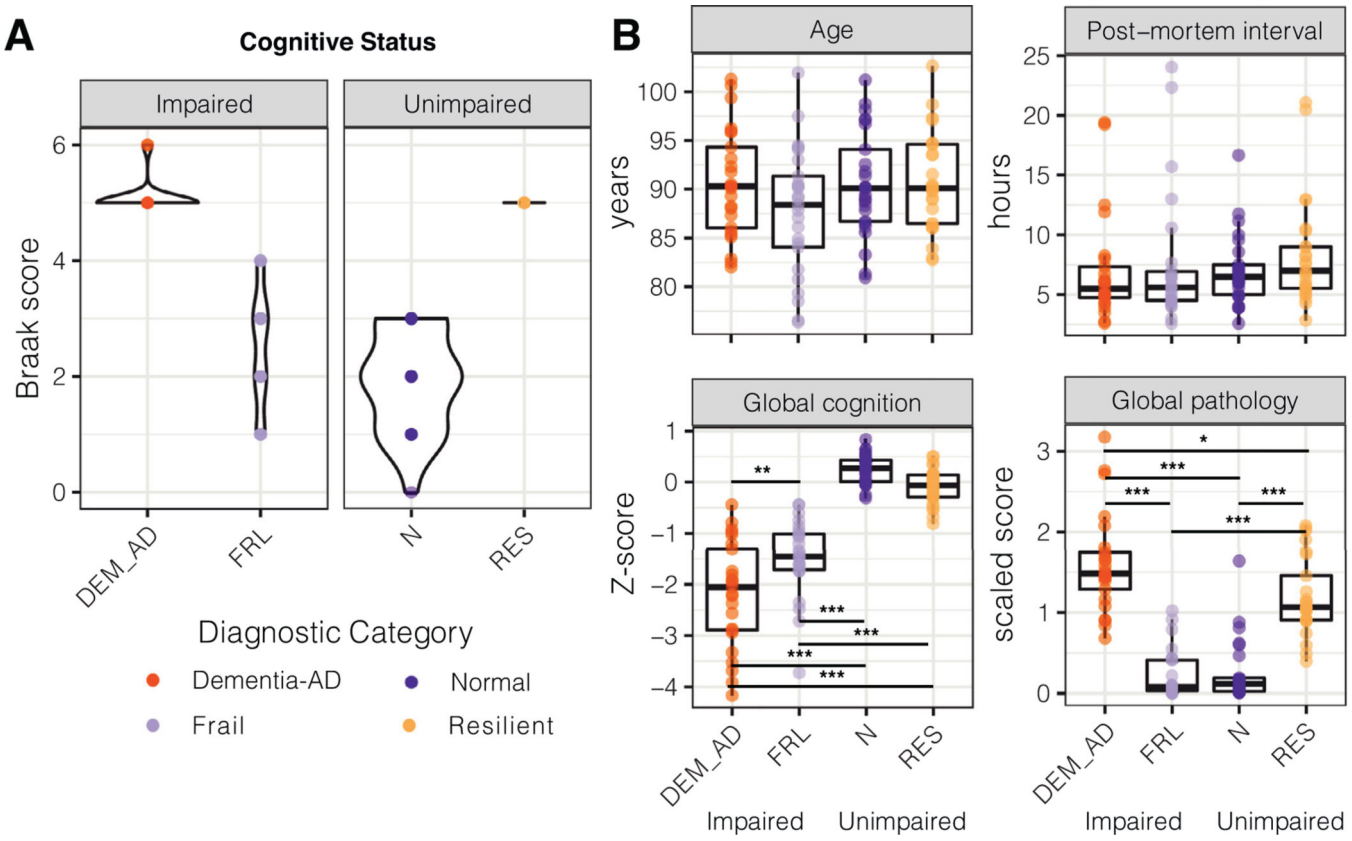

Fig. 1.

One hundred subject samples were categorized based on their levels of AD pathology and cognitive performance into a well-balanced study cohort (A) Samples were divided into 4 groups by Braak score (Braak > 4 high pathology, Braak ≤ 4 low pathology) and clinical diagnosis of the presence of dementia-level cognitive impairment (n = 25 per group). (B) Age and post-mortem interval were well balanced across all diagnostic groups. Global cognition score (A Z-score transformed summary score encompassing a battery of 21 different cognitive tests assessing the different domains of cognition) at last valid visit was significantly higher in Normal and Resilient subjects compared to Dementia-AD and Frail subjects. There was a small but significant difference in global cognition score between Dementia-AD and Frail subjects. Global pathology score (a Z-score transformed score accounting for diffuse and neuritic plaques, and neurofibrillary tangles) was significantly higher in Dementia-AD and Resilient subjects than Normal and Frail Subjects. There was a small but significant difference in global pathology between Dementia-AD and Resilient subjects. Between group significance was defined by one-way ANOVA followed by Tukey post-hoc testing, (*adjusted $p < 0.05$, **$p < 0.01$, ***$p < 0.001$). (For interpretation of the references to color in this figure legend, the reader is referred to the Web version of this article).

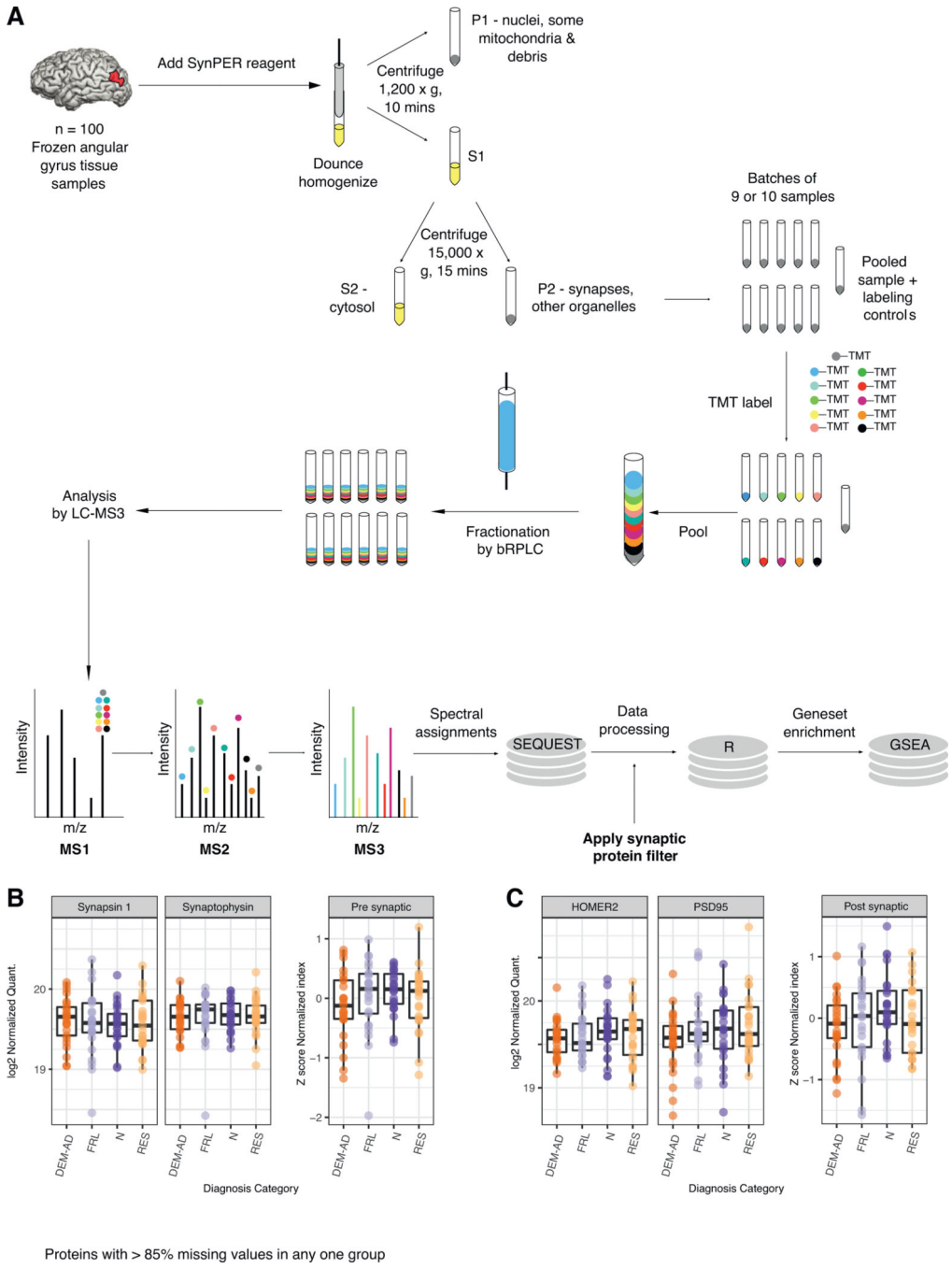

Fig. 2.

Fractionated LC-MS3 was used to assess synaptic protein enriched fractions from the angular gyrus. (A) Schematic diagram showing experimental workflow. Cortical grey matter samples from the angular gyrus (Brodmann Area 39) were fractionated to enrich for synaptic proteins using the SynPER reagent and low speed centrifugation. Synaptic protein fractions were Tandem Mass Tag (TMT) labelled, pooled, and offline fractionated into twelve fractions. Fractions were analyzed by liquid chromatography mass spectrometry (LC-MS3). Spectra were assigned using the SEQUEST algorithm and quantified using a custom

software pipeline. Proteins were filtered using a synaptic protein inclusion list, and analysis and figures were prepared in R and using the GSEA java applet. (B) Abundance of established pre-synaptic markers across the four diagnostic groups suggested there was no significant volume artefact arising from gross synapse loss between groups. The pre-synaptic summary plot is a Z-score normalized composite of SYT1, NRZN3, SNAP25, SYN2, STX1A, STX1B, SLC17A6, SYN1, and SYP. (C) Abundance of established post-synaptic markers across the diagnostic groups suggest there was no volume artifact arising from gross synapse loss between groups. The post-synaptic summary plot is a Z-score normalized composite of EPHB1, DLG3, DLG4 (PSD95), HOMER2, NLGN1, NLGN2, and SHANK1. For interpretation of the references to color in this figure legend, the reader is referred to the Web version of this article

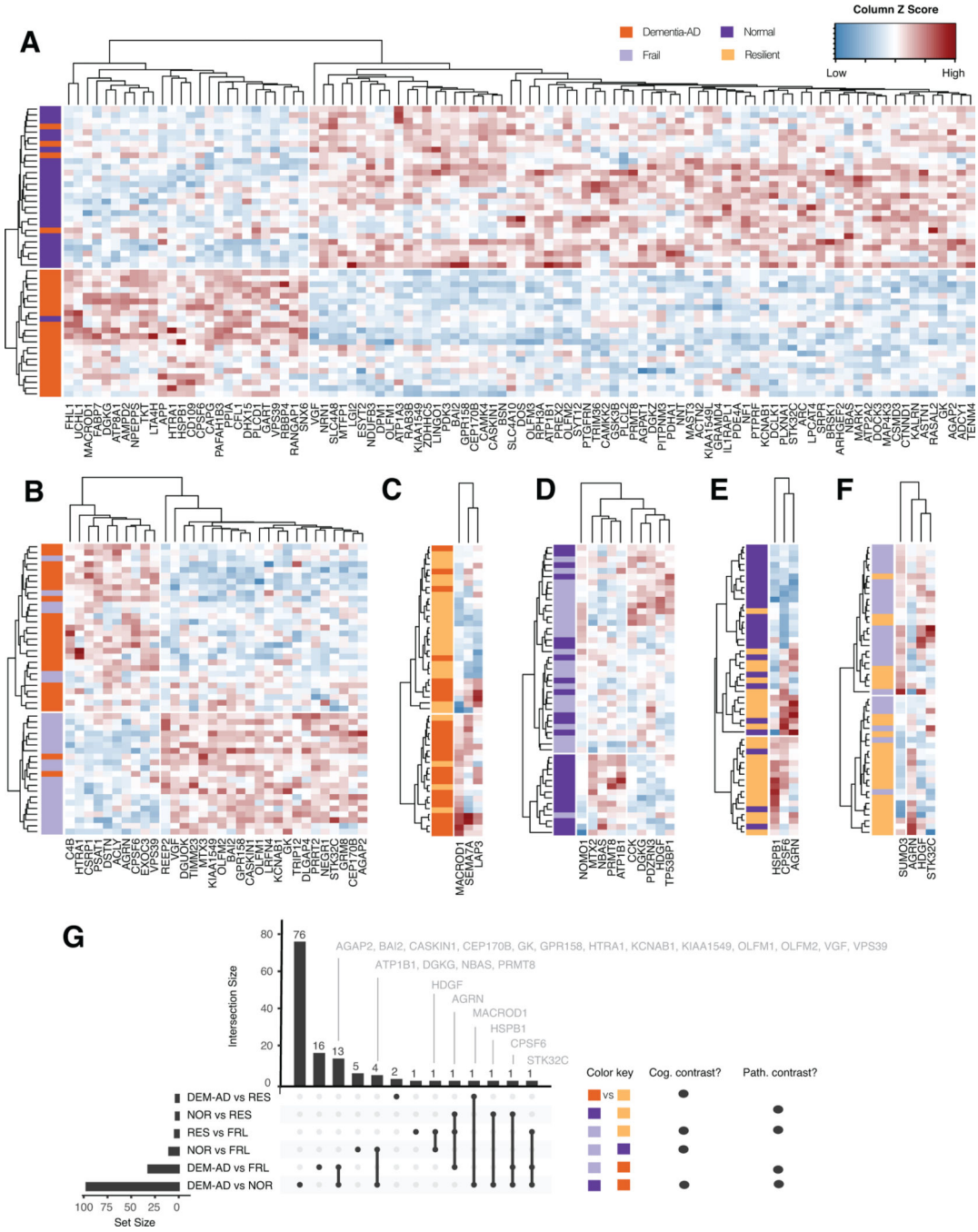

Fig. 3.

In total, 123 unique proteins were differentially expressed between diagnostic groups, with no clear sign of a volume artefact from synapse loss in Dementia-AD subjects. (A) Heatmap of differentially expressed proteins between Dementia-AD and Normal cases shows 97 proteins. Clustering on abundance of these 97 proteins produces good separation between Dementia-AD and Normal subjects. Heatmap of differentially expressed proteins between (B) Dementia-AD and Frail, (C) Dementia-AD and Resilient, (D) Normal and Frail, (E) Normal and Resilient, and (F) Resilient and Frail subjects. (G) Upset plot shows the

intersection of proteins common to multiple comparisons. Vertical lines join contrasts that shared the same set of proteins. For example, 13 proteins were significant in both the Dementia-AD versus Frail and Dementia-AD versus Normal contrasts. (For interpretation of the references to color in this figure legend, the reader is referred to the Web version of this article).

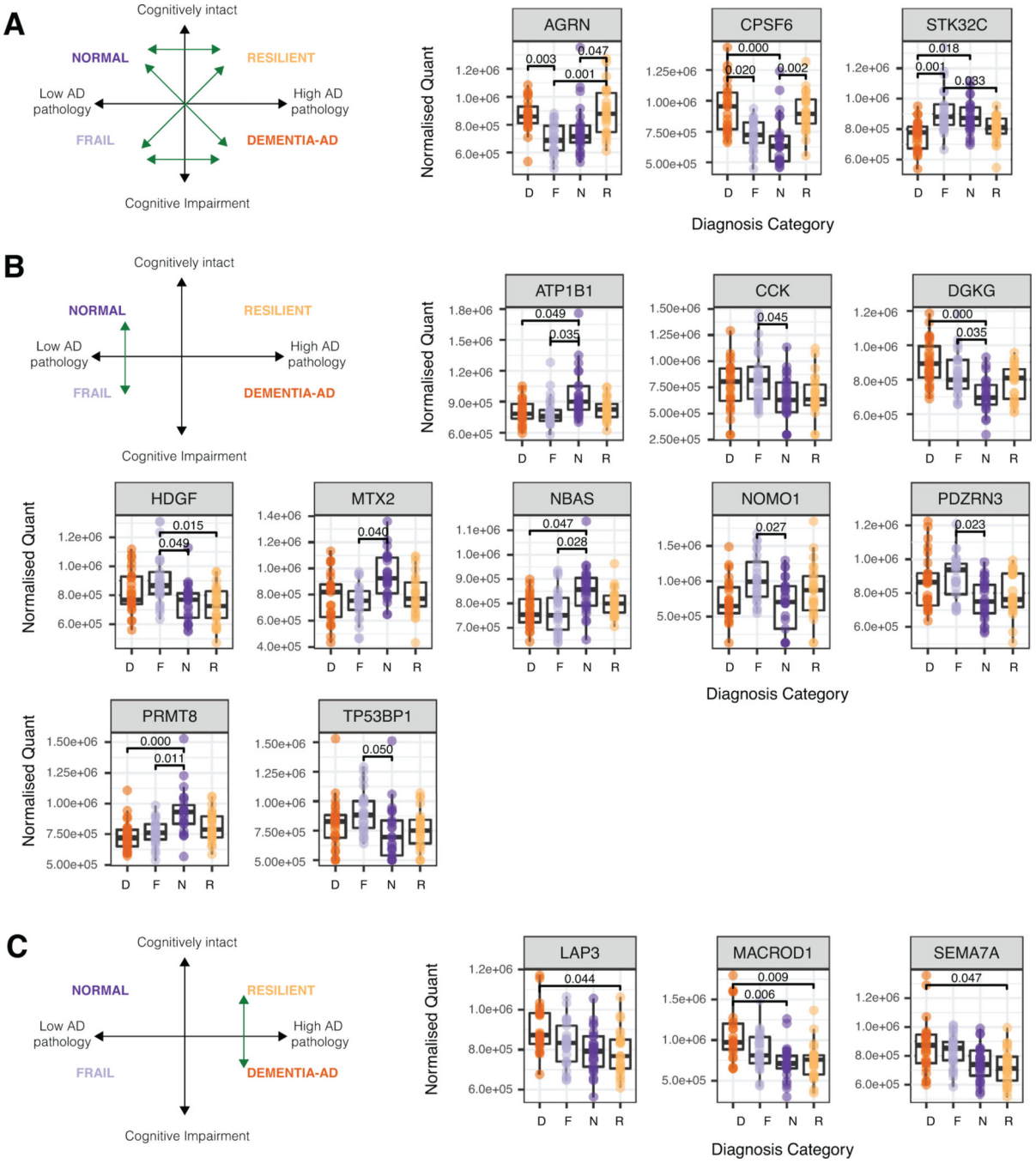

Fig. 4.

A small number of proteins tracked frequently with pathological contrasts or a subset of cognitive contrasts. (A) Box plots to illustrate the three proteins that were significant in three of the four pathological contrasts. The green arrows on the contrast schematic show the contrasts that the proteins were significantly associated with. Adjusted *p*-values are given to three significant figures. (B) Box plots to illustrate proteins that were significant in the Normal versus Frail contrast. (C) Box plots to illustrate proteins that were significantly associated with the Dementia-AD versus Resilient contrast. (For interpretation of the

references to color in this figure legend, the reader is referred to the Web version of this article).

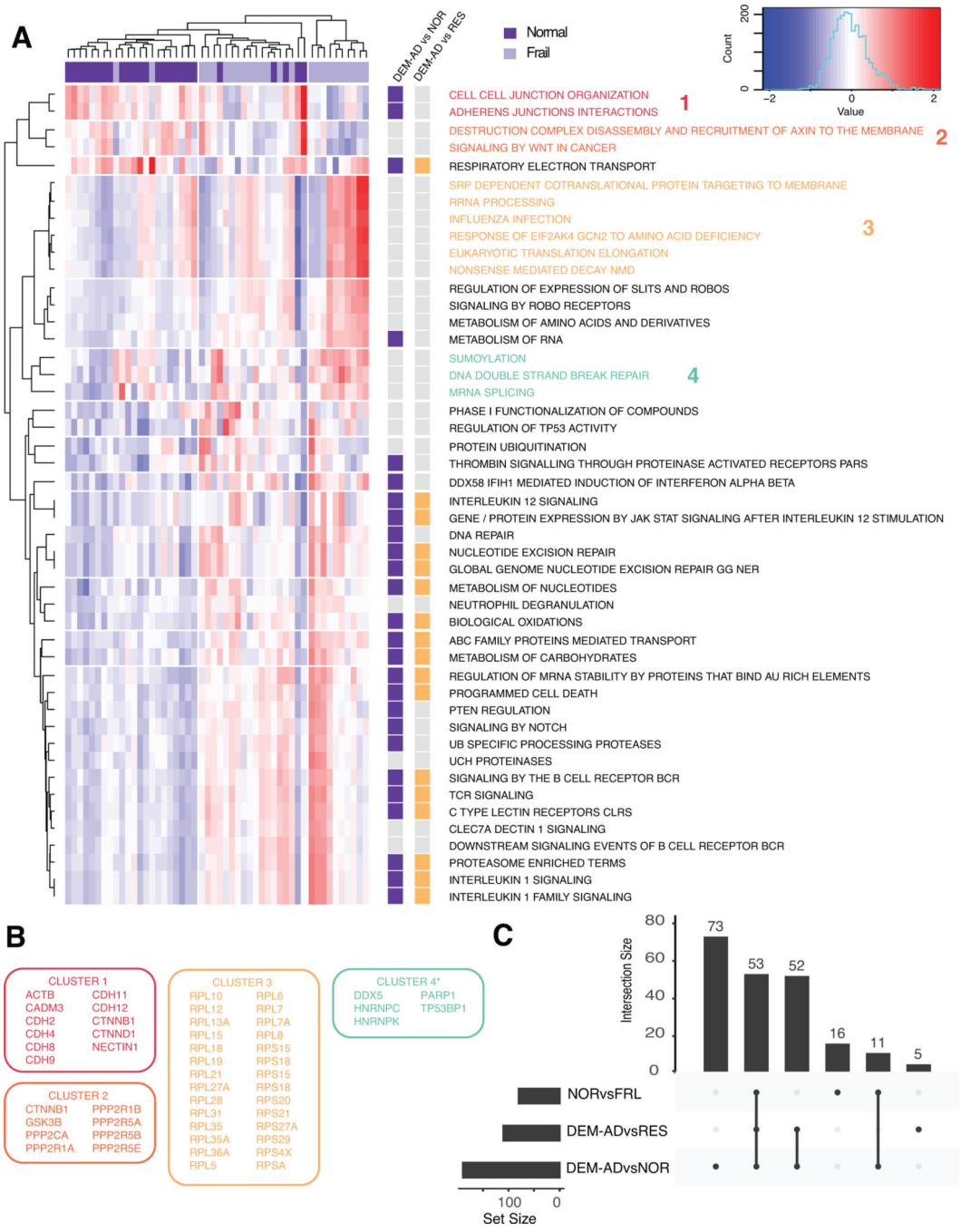

Fig. 5.

Summary of Gene Set Enrichment Analysis from Frail versus Normal subjects shows that Frail subject exhibit of subset of the features of Dementia-AD. (A) Heatmap shows nominally significant (padj relaxed to < 0.10) clustered REACTOME protein categories from the Frail versus Normal comparison. Comparison with the significant terms from other cognitive contrasts is shown alongside. Clusters of proteins are highlighted by color, (B) lists the proteins driving each highlighted cluster. For clusters without an asterisk in the title, all proteins are present in all terms in that cluster. For those with the asterisk, proteins are

present in the majority of terms. (C) Upset plot shows the number of protein categories shared between each cognitive contrast. The majority of the terms that reach nominal significance in the Normal versus Frail contrast are shared with the Dementia-AD versus Resilient and Dementia-AD versus Normal contrasts, with Frail subjects behaving similarly to Dementia-AD. Only 5 protein categories are unique to the Dementia-AD versus Resilience contrast. Vertical lines join contrasts that shared the same set of proteins. The Upset plot counts categories that were collapsed into the “Proteasome Enriched” term as their initial individual categories. (For interpretation of the references to color in this figure legend, the reader is referred to the Web version of this article).

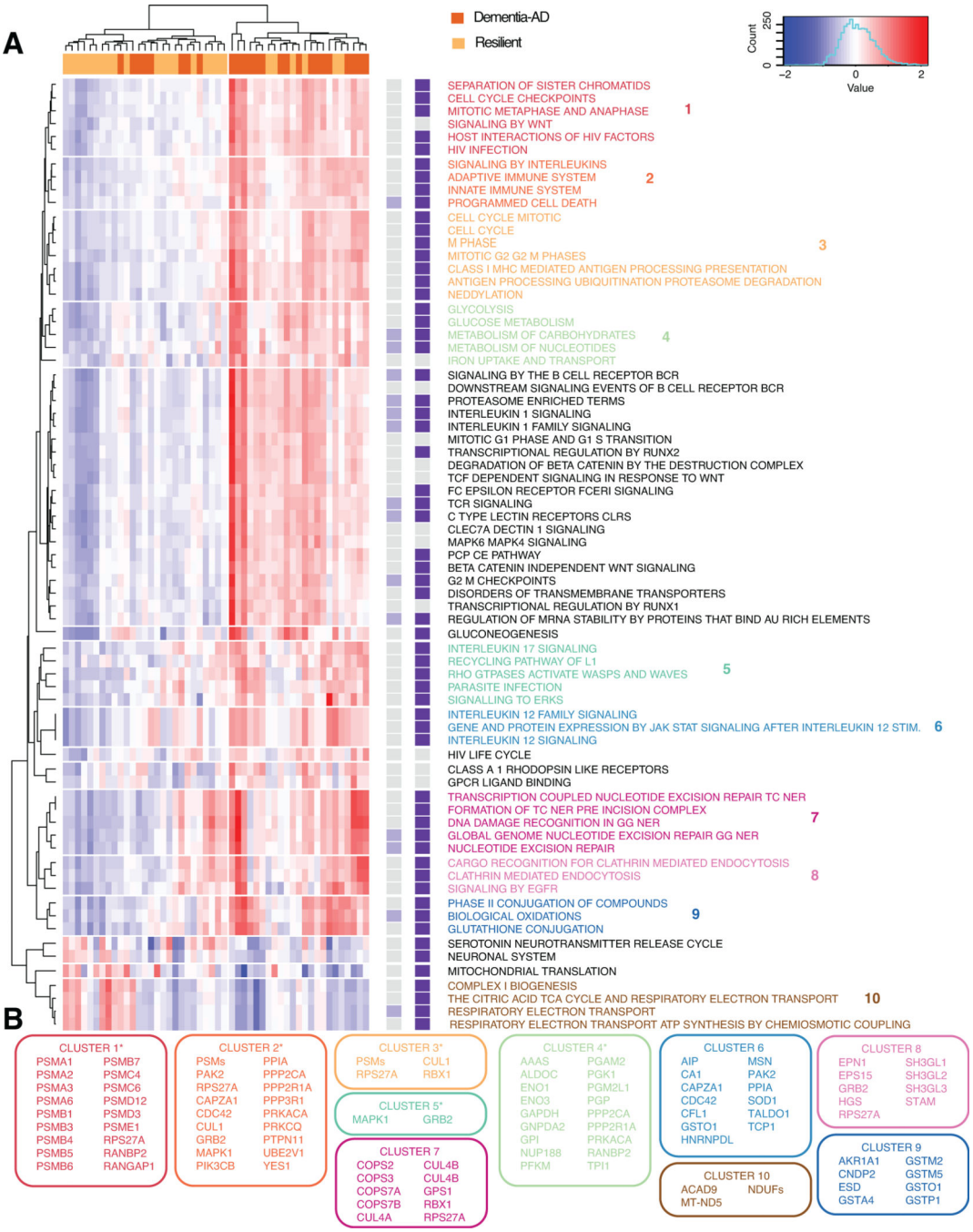

Fig. 6.

Summary of Gene Set Enrichment Analysis from Dementia-AD versus Resilient samples shows substantial overlap with the Dementia-AD versus Normal contrast. Heatmap shows FDR significant (padj < 0.05) clustered REACTOME protein categories from the Dementia-AD versus Resilient comparison. There is substantial overlap between these protein categories and those significant in the Dementia-AD versus Normal comparison. Clusters of proteins are highlighted by color, (B) lists the proteins driving each highlighted cluster. For clusters without an asterisk in the title, all proteins are present in all protein categories in that

cluster. For those with the asterisk, proteins are present in the majority of protein categories. (For interpretation of the references to color in this figure legend, the reader is referred to the Web version of this article).

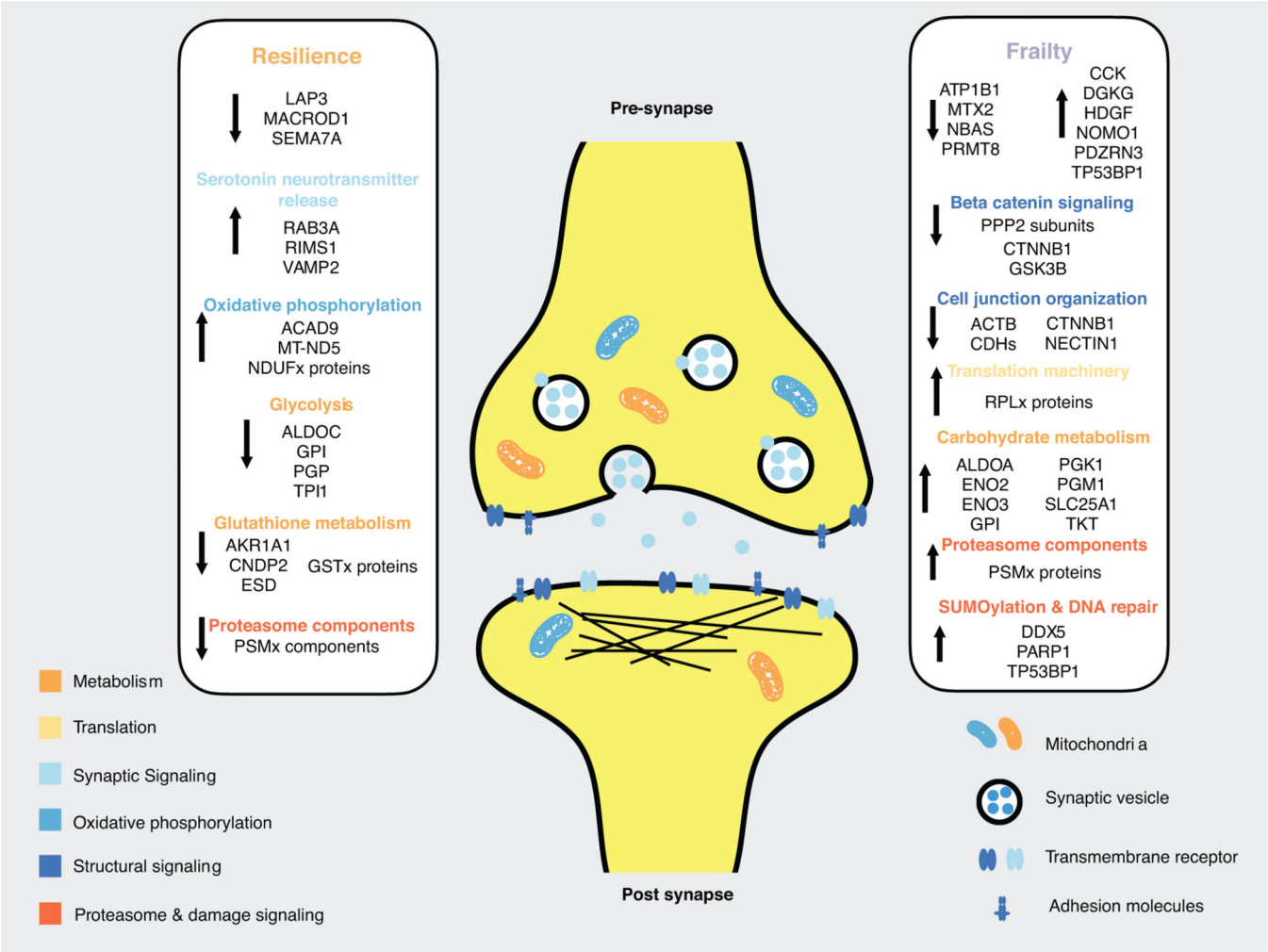

Fig. 7.

Summary cartoon showing proteins and REACTOME protein categories associated with Frailty or Resilience, and their putative cellular locations. The black arrows next to protein groups show the direction of effect; for example, Serotonin neurotransmitter release is enriched in Resilience. Protein categories are color coded according to their over-riding function and putative cellular location. (For interpretation of the references to color in this figure legend, the reader is referred to the Web version of this article).

Table 1

Summary demographics of cases. Data is presented as mean (standard deviation). See Supplementary Table 1 for individual sample demographic data. * MMSE = Mini Mental State Examination. The global cognition score is a ROSMAP cohort-wide Z-score normalized summary value encompassing a battery of 21 different cognitive tests assessing 5 domains of cognition (episodic memory, semantic memory, working memory, perceptual orientation, and perceptual speed). The global pathology score is a quantitative summary score of amyloid and tau pathology burden averaged across 5 brain regions, presented as a ROSMAP cohort-wide Z-score.

	Dementia-AD	Frail	Normal	Resilient
N	25	25	25	25
Age (years)	90.6 (5.5)	87.7 (6.5)	90.5 (5.4)	90.8 (5.1)
% male	42	48	44	44
Education (years)	16.2 (3.2)	16.7 (3.5)	17.0 (3.7)	16.3 (3.8)
Post-mortem interval (hours)	7.0 (4.4)	7.5 (5.6)	7.0 (3.0)	8.3 (4.5)
MMSE * (maximum score 30)	11.0 (9.5)	17.6 (8.5)	28.0 (1.6)	27.5 (1.8)
Last valid global cognition (Z-score)	−2.2 (1.0)	−1.5 (0.7)	0.3 (0.3)	−0.1 (0.3)
Braak score	5.1 (0.3)	2.5 (1.0)	1.9 (0.9)	5.0 (0)
Global pathology (Z-score)	1.6 (0.6)	0.2 (0.3)	0.3 (0.4)	1.2 (0.5)

Table 2

Summary of proteins significantly (padj < 0.05) associated with each explanatory variable. No proteins were associated with level of education

Variable	Increase	Decrease
Age	8	1
Dx Dementia-AD vs Normal	26	71
Dx Frail vs Dementia-AD	22	10
Dx Frail vs Normal	6	4
Dx Frail vs Resilient	3	1
Dx Resilient vs Dementia-AD	0	3
Dx Resilient vs Normal	3	0
Post-mortem Interval	6	54
Sex Male vs Female	11	23